Running Head: RAPID ADAPTIVE RADIATION OF HELICONIUS

Title: Multilocus Species Trees Show the Recent Adaptive Radiation of the Mimetic *Heliconius* Butterflies

Krzysztof M. Kozak[1*], Niklas Wahlberg[2], Andrew Neild[3], Kanchon K. Dasmahapatra[4,] James Mallet[5], Chris D. Jiggins[1,6]

[1]*Butterfly Genetics Group, Department of Zoology, University of Cambridge, CB2 3EJ Cambridge UK*

[2]*Laboratory of Genetics, Department of Biology, University of Turku, 20014 Turku, Finland*

[3] *Nr 8 Old Park Ridings, Grange Road, London N21 2EU, UK*

[4]*Department of Biology, University of York, YO10 5DD Heslington, York, UK*

[5]*Department of Organismic and Evolutionary Biology, Harvard University, Cambridge, MA 02138, USA*

[5]*Smithsonian Tropical Research Institute, Panama City, Panama*

**Corresponding author:* kk443@cam.ac.uk*, Phone: 00441223336644*

ABSTRACT

Müllerian mimicry among Neotropical Heliconiini butterflies is an excellent example of natural selection, and is associated with the diversification of a large continental-scale radiation. Some of the processes driving the evolution of mimicry rings are likely to generate incongruent phylogenetic signals across the assemblage, and thus pose a challenge for systematics. We use a dataset of 22 mitochondrial and nuclear markers from 92% of species in the tribe to re-examine the phylogeny of Heliconiini with both supermatrix and multi-species coalescent approaches, characterise the patterns of conflicting signal and compare the performance of various methodological approaches to reflect the heterogeneity across the data. Despite the large extent of reticulate signal and strong conflict between markers, nearly identical topologies are consistently recovered by most of the analyses, although the supermatrix approach fails to reflect the underlying variation in the history of individual loci. The first comprehensive, time-calibrated phylogeny of this group is used to test the hypotheses of a diversification rate increase driven by the dramatic environmental changes in the Amazonia over the past 23 million years, or changes caused by diversity-dependent effects on the rate of diversification. We find that the tribe Heliconiini had doubled its rate of speciation around 11 Ma and that the presently most speciose genus *Heliconius* started diversifying rapidly at 10 Ma, likely in response to the recent drastic changes in topography of the region. Our study provides comprehensive evidence for a rapid adaptive radiation among an important insect radiation in the most biodiverse region of the planet.

Keywords: multispecies coalescent, speciation rate, incongruence, mimicry, Lepidoptera, Amazonia, Miocene

Visual mimicry provides an excellent system in which to study the origins of biodiversity, as the targets of selection are clearly identifiable and the role of natural selection in promoting adaptation and ultimately speciation can be directly observed (Bates 1863; Benson 1972; Mallet and Barton 1989; Sherratt 2008; Pfennig 2012). Studies of mimetic assemblages have been instrumental in explaining many biological phenomena, ranging from reproductive isolation (McMillan et al. 1997; Jiggins et al. 2001; Merrill et al. 2012) to genetics of adaptation (Benitez-Vieyra et al. 2007; Baxter et al. 2009; Jones et al. 2012), and including prominent examples from vertebrates (Brodie III and Brodie Jr 2004, Wright 2011), arthropods (Ceccarelli and Crozier 2007, Janzen et al. 2010, Hines and Williams 2012), plants (Benitez-Vieyra et al. 2007), and microbes (Elde and Malik 2009).

Testing hypotheses regarding the evolution of mimicry depends heavily on our knowledge of systematic relationships between the participating taxa, particularly where mimics are closely related. Phylogenetic comparative approaches have been used to address questions such as concerted coevolution of Müllerian co-mimics in catfish (Wright 2011), advergence due to directional selection in Batesian mimicry of spiders (Ceccarelli and Crozier 2007) and selection on imperfect mimics among the hoverflies (Penney et al. 2012). Unfortunately, both hybridisation driven by strong selection on adaptive loci and rapid radiation leading to incomplete lineage sorting are likely to be common in mimetic systems (Savage and Mullen 2009; Kubatko and Meng 2010; Kunte et al. 2011; Zhang et al. 2013) and can significantly interfere with the estimation of phylogenies (Maddison and Knowles 2006; Linnen and Farrell 2008; Edwards 2009; Anderson et al. 2012).

We use the Neotropical butterfly tribe Heliconiini (Nymphalidae: Heliconiinae) to explore the problem of phylogeny estimation in a Müllerian mimetic group and investigate the link between the dynamics of speciation and macroevolutionary factors. Heliconiini are arguably the most thoroughly-researched example of microevolution in the Neotropics, the most biodiverse region of the world (Hoorn et al. 2010). They comprise the genus *Heliconius* and nine smaller genera,

providing a spectacular example of a radiation where speciation is frequently caused by mimicry of aposematic patterns directed against avian predators (Jiggins et al. 2001; Arias et al. 2008; Merrill et al. 2012). The system has provided an excellent example for the study of convergence from both genomic and organismal perspective (e. g. Duenez-Guzman et al. 2009; Hines et al. 2011; Bybee et al. 2012; Heliconius Genome Consortium 2012; Martin et al. 2012, 2013; Pardo-Díaz et al. 2012; Jones et al. 2013; Nadeau et al. 2013; Supple et al. 2013). The clade presents an opportunity for comparative studies of many unique traits, including larval and imaginal sociality (Beltrán et al. 2007), pupal mating (Estrada et al. 2011), pollen feeding (Cardoso and Gilbert 2013), or close association with varying numbers of Passifloraceae host plants (Brown 1981; Merrill et al. 2013). The ongoing proliferation of comparative molecular and genomic studies on the diversity of genes regulating vision (Pohl et al. 2009), chemosensation (Briscoe et al. 2013) and cyanogenesis (Chauhan et al. 2013) makes a stable molecular phylogeny especially desirable.

An unusual feature of *Heliconius* is the prevalence and importance of gene flow and hybridisation, leading to a controversy over the validity of traditional species concepts in the clade (Beltrán et al. 2002; Mallet et al. 2007). At least 26% of all species of Heliconiini occasionally produce hybrids in the wild (Mallet et al. 2007), and *H. heurippa* has resulted from homoploid hybrid speciation from parental forms diverged millions of years ago (Mavárez et al. 2006; Jiggins et al. 2008; Salazar et al. 2010). Genome sequencing has shown that mimetic diversity in the *H. melpomene* and silvaniform clades is also explained by adaptive introgression of genes regulating the aposematic wing patterns (Heliconius Genome Consortium 2012; Pardo-Díaz et al. 2012), and seemingly neutral gene flow is widespread, influencing as much as 40% of the genome between *H. melpomene* and *H. cydno* (Martin et al. 2013).

A large body of recent work has been devoted to the issue of incongruence between the species tree (the true speciation history) and the gene trees evolving within (Anderson et al. 2012; Cutter 2013). The traditional approach of concatenating the total genetic evidence into a supermatrix in order to obtain a global estimate of the predominant phylogenetic signal and hidden

support (Gatesy and Baker 2005), without consideration for the heterogeneity of individual partitions, has been to some extent superseded by multispecies coalescent (MSC) techniques (reviewed in: Edwards 2009; Knowles and Kubatko 2010; Anderson et al. 2012; Cutter 2013; Leaché et al. 2013). The majority of the new MSC algorithms are intended to model at least some of the sources of heterogeneity between different markers, most frequently focusing on the problem of incomplete lineage sorting (e.g. Maddison and Knowles 2006; Heled and Drummond 2010), sometimes addressing hybridisation (e.g. Gerard et al. 2011; Yu et al. 2011), and in at least one case modelling discordance without specifying its potential source (Larget et al. 2010). Although the supermatrix approach remains popular and serves as an effective approximation of the species diversification history in most cases, its ability to properly assess the degree of statistical support for phylogenies has been brought into question and contrasted with the potential of the MSC techniques to assess confidence more realistically (Edwards 2009; Knowles and Kubatko 2010). Heliconiini are an especially interesting subject for a systematic study, where the purported robustness of MSC tools to gene flow and other sources of incongruence can be tested with real data and used to evaluate support in the light of underlying heterogeneity of the phylogenetic signal.

Heliconiini systematics has a long history, starting with early morphological work (Emsley 1965; Brown 1981; Penz 1999), through allozymes (Turner et al. 1979) and a combination of morphological and RNA-restriction data (Lee et al. 1992), to studies based on the sequences of mitochondrial and nuclear markers (Brower 1994b; Brower and Egan 1997; Beltrán et al. 2002, 2007; Cuthill and Charleston 2012). The most comprehensive study to date by Beltrán et al. (2007) attempted to address some of the difficulties by incorporating many taxa (38 of 46 *Heliconius*, 59 of 78 Heliconiini), considering two individuals of most species, and sequencing two mitochondrial (*CoI/II*, *16S*) and four nuclear markers (*EF1α*, *Wg*, *Ap*, *Dpp*). However, this dataset is still potentially inadequate to address the challenges posed by Heliconiini systematics, as three of the loci (*16S*, *Ap*, *Dpp*) were only sequenced for 12 representative species. Among the other three markers, 65% of the variable sites resided in the fast-evolving mitochondrial partition *CoI/II*,

raising the possibility that the inferred relations are largely driven by the historical signal of the matriline. The proposed relationships between the basal genera of the tribe were poorly supported and the relationships between *Heliconius*, *Eueides* and the other eight genera was not resolved, as might be expected if most of the data comes from a fast-evolving partition. Importantly, the individual data partitions were analysed in concatenation, as the debate on the species tree-gene tree incongruence was in its early stages at the time. Despite these shortcomings, Beltrán and colleagues confirmed that the morphological and behavioural characteristics of the major clades do not correspond directly to their evolutionary history and that the traditionally recognised genera *Laparus* and *Neruda* are most likely nested within the crown genus *Heliconius*.

The importance of Müllerian mimicry as a driver of individual speciation events has been well-established (Mallet et al. 1998; Mallet and Joron 1999; Jiggins 2008) whereas the macroevolutionary processes governing the evolution of the group have been largely neglected in empirical studies (but see Etienne et al. 2012; Rosser et al. 2012). Precise understanding of the evolution of the Müllerian mimicry rings as well as associated processes such as hybridisation, requires knowledge of the relative timing of the divergence events and motivated the most widely-cited study of the molecular clock in Arthropoda (Brower 1994a). Mallet et al. (2007) used a relaxed clock procedure to adjust the original branch lengths based on the *CoI/II* alignment. However, some of the relations were left unresolved, and the sequences were not partitioned into fast and slow-evolving codon positions, which can result in inflated age estimates (Brandley et al. 2011).

Most importantly, the first dated phylogeny of Heliconiini is not calibrated to an absolute standard, making it impossible to make inferences about the relation of the diversification process and the contemporaneous geological and climatic events. The cumulative results of over 200 systematic studies demonstrate that most South American tropical clades have experienced periods of significantly elevated net diversification rate in response to Andean orogenesis, alterations in the hydrology and sediment dynamics of the present-day Amazon Basin, as well as local and global

154 climatic changes (Hoorn et al. 2010; Turchetto-Zolet et al. 2013). These processes can result in
155 allopatry of incipient lineages, or in creation of new ecological niches and change to the species-
156 level carrying capacity of the environment leading to ecological speciation (Brumfield and Edwards
157 2007; Hoorn et al. 2010). A recent comparative study suggests that the majority of *Heliconius*
158 lineages originated in the North-Eastern Andes and spread to other parts of the continent (Rosser et
159 al. 2012). Three periods stand out as potentially critical in the history of Heliconiini as the times
160 when orogenic, hydrologic and climatic events would have created new habitats and altitudinal
161 gradients. The first phase of the intense Andean uplift, taking place 23 Ma, was also the start of the
162 great marine incursion into the North of the continent, separating the incipient mountain range from
163 the Eastern plateaus (Gregory-Wodzicki 2000; Solomon et al. 2008; Hoorn et al. 2010). 12.4 Ma
164 marked the end of the Mid-Miocene Climatic Optimum and the onset of global cooling (Lewis et al.
165 2007), which likely led to the reduction and separation of the rainforest areas by savannas
166 unsuitable for many Heliconiini (Jaramillo et al. 2011). Coincident was the second stage of rapid
167 Andean orogeny 12 Ma, strongly changing the elevation gradients in the Central and Eastern sectors
168 (Gregory-Wodzicki 2000), and followed shortly by the entrenchment of the Amazon in its modern
169 course 10 Ma, and a gradual expansion of the rainforest in place of the retreating wetlands during
170 the next 3 Myr (Hall and Harvey 2002, Figueiredo 2009, Hoorn 2010). Finally, the Eastern
171 Colombian Cordillera uplifted in the last burst 4.5 Ma and the Isthmus of Panama connected at least
172 3 Ma, possibly changing the patterns of isolation between various populations (Hill et al. 2013).
173 Hence we can hypothesise that the diversification rate of Heliconiini increased during the periods of
174 intensive Andean uplift around 23, 12 and 4.5 Ma.
175
176 *Aims of the Study*
177 Here we aim to resolve the species tree of the Heliconiini radiation and generate a dataset
178 including virtually all of the currently valid species in the tribe, sampling intraspecific diversity
179 across the range of many of the species. We include information from 20 nuclear and two

mitochondrial markers, as well as the whole mitochondrial sequence of select species. The exonic markers comprise both autosomal and Z-linked loci, chosen to represent a sampling of chromosomes and a range of evolutionary rates, from fast-evolving mitochondrial genes (e.g. *CoI/II*) to more slow evolving nuclear loci (e.g. *Wg*). We apply a wide range of phylogenetic methods to reconstruct the species tree, including supermatrix, coalescent and network approaches, which allow us to assess the strength of the underlying signal of speciation. The power of our combined approach is harnessed to detect the incongruence between markers, likely to arise from the complex population-level processes acting in a radiation of Müllerian co-mimics. We elucidate the importance of marker heterogeneity for the final assessment of systematic relationships, while realistically estimating the support values for our chosen topology. A robust estimate of the relationships between 92% of the species and multiple outgroups makes it possible to date the time of individual divergence events with confidence, providing input for an analysis of diversification dynamics. The calibrated chronogram is used to test our hypothesis of diversification rate increase at times of dramatic environmental changes in the Andes and Amazonia, as well as the previous suggestions of diversity-dependent cladogenesis in Heliconiini (Fordyce 2010; Etienne et al. 2012). We thus present a comprehensive study of macroevolutionary dynamics in a mimetic system that has been studied intensively at the microevolutionary level.

MATERIALS AND METHODS

Taxon Sampling

We sampled 180 individuals, including 71 of the 78 species in all genera of Heliconiini and 11 outgroup species. The specimens came primarily from our collection at the University of Cambridge, with additional specimens shared by museums and private collectors (Online Appendix 1). We included five outgroup species from the sister tribe Acraeini (Wahlberg et al. 2009) and three from the related genus *Cethosia*. The diverse analyses used in this paper require different sampling designs and the demands of all the techniques cannot be easily accommodated in a single dataset. For example, the network analysis based on nucleotide distance produced much better supported and resolved trees when the 95% or more incomplete data from historical specimens were not used, whereas the various multi-species coalescent techniques required the use of at least two individuals per species and had to be based only on taxa with intraspecific sampling (Fulton and Strobeck 2009; Heled and Drummond 2010). Thus we distinguish four datasets. The complete data matrix includes all the data. The core dataset excludes 14 individuals represented solely by short DNA fragments from historical specimens. The single-individual dataset includes both modern and historical specimens, but with only the single best-sequenced individual per taxon. Finally, the *BEAST matrix contains only the 17 species of *Eueides* and *Heliconius* with extensive sampling of multiple representatives of each species.

DNA Sequencing

We used 20 nuclear and two mitochondrial loci as markers (Table 1; Online Appendix 1), exceeding the number of loci considered sufficient for most phylogenetic problems (Gatesy et al. 2007). The selection includes the three classic molecular markers for Lepidoptera (*CoI/II*, *EF1α*, *Wg*), two markers proposed by Beltrán et al. (2007)(*16S*, *Dpp*), eight new universal markers proposed by Wahlberg and Wheat (2008) (*ArgK*, *Cad*, *Cmdh*, *Ddc*, *Idh*, *Gapdh*, *Rps2*, *Rps5*) and

nine highly variable loci identified by Salazar et al. (2010) (*Aact*, *Cat*, *GlyRS*, *Hcl*, *Hsp40, Lm*, *Tada3*, *Trh*, *Vas*). Additional *Heliconius*-specific primers were designed for *Cmdh*, *Gapdh* and *Idh*. Details of the primers and PCR cycles are listed in the Online Appendix 2. For most species, sequences of the three basic markers for multiple individuals were already published (Brower 1997; Beltrán et al. 2007; Wahlberg et al. 2009; Salazar et al. 2010), and data for 26 individuals came exclusively from GenBank (Online Appendix 1).

We generated Sanger sequences for 103 specimens (Online Appendix 1). DNA was isolated from approximately 50 µg of thorax tissue using the DNeasy Blood & Tissue kit (Qiagen, Manchester, UK). PCR was carried out in a total volume of 20 µl, containing 1x Qiagen Taq buffer (Manchester, UK), 2.5 mM $MgCl_2$, 0.5 µM of each primer, 0.2 mM dNTPs, 1 unit bovine serum albumin, 0.5 unit Qiagen Taq-Polymerase and 1 µl of the DNA extract. The following program was executed on a G-Storm cycler (Somerton, UK): denaturation 5 minutes at 94°C; 35 cycles of 30 seconds at 94°C, 30 seconds at the annealing temperature and 90 seconds at 72°C; final extension for 10 minutes at 72°C. The results were visualised by electrophoresis in 1.5% agarose gel stained with 1% ethidium bromide. PCR products were cleaned using the ExoSAP-IT system (USB, Cleveland, Ohio): 60 minutes at 37°C; 20 minutes at 80°C. We used gel purification with the Nucleo Spin Extract II kit (Macherey-Nagel, Dueren, Germany) as needed. Sanger sequencing reaction was carried out with the BigDye Terminator v. 3.1 (AB, Foster City, California: 2 minutes at 94°C; 25 cycles of 10 seconds at 94°C, five seconds at 50°C and four minutes at 60°C. The products were sequenced with the ABI 3730xl DNA Analyzer at the Sequencing Facility, Department of Biochemistry, University of Cambridge. We manually inspected the traces in CodonCode v. 4.0.4 using PHRED for quality assessment (CodonCode Corporation 2012).

At the time of our Sanger sequencing effort, whole genome data generated for other studies became available from 57 individuals in 27 common species (Heliconius Genome Consortium 2012; Briscoe et al. 2013; Supple et al. 2013; Dasmahapatra and Mallet, unpublished) (Online Appendix 1). 100 base pair reads were generated using the Illumina Genome Analyzer II and HiSeq

2000 platforms with insert size of 300-400 bp. We performed *de novo* assembly of the short reads in the program Abyss v. 1.3 (Simpson et al. 2009). Based on previous studies (Salzberg et al. 2012; Briscoe et al. 2013) and preliminary results (S. Baxter, *pers. comm.*), we chose k-mer length of 31, minimum number of pairs n=5 and minimum mean coverage c=2 as optimal settings. The 20 nuclear markers were mined from the assemblies by megaBLAST (Camacho et al. 2009) in Geneious v. 5.5.1 (Biomatters Ltd 2012) using reference sequences from the *Heliconius melpomene* genome. The quality of the recovered sequences was assessed by alignment to previously generated amplicon sequences of the same loci from the same individuals.

Mitochondrial sequences could not be recovered by *de novo* methods, presumably because the large number of reads from the highly abundant mitochondrial DNA contained a high enough number of erroneous sequences to interfere with the assembly. We reconstructed whole mitochondrial genomes of 27 species by mapping to the *Heliconius melpomene* reference (The *Heliconius* Genome Consortium, 2012), using the default settings in the Genomics Workbench v. 5.5.1 (CLCBio 2012). This data was analysed separately from the 21 locus mixed nuclear-mitochondrial alignment. All the original sequences were deposited in GenBank (Accession numbers – data in submission; Online Appendix 1).

DNA Sequencing: Historical Specimens

Short fragments of *CoI/II* and *EF1α* were sequenced from historical specimens up to 150 years of age, obtained from museum and private collections (Online Appendix 1) and processed in a vertebrate genetics laboratory to reduce the risk of contamination. Instruments and surfaces were cleaned with 5% bleach and irradiated with UV for 30 minutes prior to use. One to two legs were washed in water, immersed in liquid nitrogen in a test tube for 30 seconds and ground up, followed by an extraction into 20 µl of buffer using the QIAmp DNA Micro Kit (Qiagen, Manchester, UK). We treated every fifth extraction and every fifth PCR as a negative control with no tissue or DNA extract. PCR reactions were carried out in a 20 µl volume using 1 unit of Platinum HiFi Taq

Polymerase (Invitrogen, London, UK) and 1x buffer, 2.5 mM $MgCl_2$, 0.5 μM of each primer, 0.2 mM dNTPs, 1 unit bovine serum albumin, sterilised DNAse-free water and 1-5 μl of the DNA extract depending on concentration. In order to accommodate shearing of DNA with time, we designed and applied PCR primers spanning short fragments of 200-300 bp (Online Appendix 2). We carried out amplification, product clean up and sequencing as above, partially accounting for possible cross-contamination by blasting the results against GenBank.

Alignment and Gene Tree Estimation

Alignments for each locus were generated in CodonCode v. 3 to account for inverted and complemented sequences, and improved using MUSCLE v. 3.8 (Edgar 2004). We visualised the alignments of the coding loci (all except the mitochondrial *16S* and the *tRNA-Leu* fragment in the *CoI/II* sequence) in Mesquite v. 2.75 (Maddison and Maddison 2011) and checked translated sequences for stop codons indicating errors. The whole mitochondrial sequences were aligned to the *Acraea issoria* and *Heliconius melpomene* references (*Heliconius* Genome Consortium 2012) using the G-INS-i algorithm in MAFFT (Katoh 2002). The number of variable and parsimony informative sites was estimated for each locus in PAUP* v. 4 (Swofford 2002). Models of sequence evolution implemented in MrBayes (Ronquist and Huelsenbeck 2003) and BEAST (Drummond and Rambaut 2007) were selected in MrModelTest v. 2.3 (Posada and Crandall 1998; Nylander 2004) based on the Akaike's AIC (Akaike 1974). Xia's test in DAMBE v. 4.0 (Xia and Xie 2001) demonstrated saturation in the third codon position of *CoI/II*. Protein-coding mitochondrial markers often display high saturation at the third codon position, potentially leading to incorrect parametrisation of substitution rate models (Brandley et al. 2011). To account for this effect, in all the subsequent analyses we treated the third codon position of the fast-evolving *CoI/II* locus as a separate partition. The Leucine tRNA (*tRNA-Leu*) fragment occurring in the middle of *CoI/II* displays very low variability and thus was included in one partition with the slower evolving first and second codon positions. Individual gene trees were estimated in MrBayes v. 3.1, using four runs of one chain, 10

million MCMC cycles sampled every 1000 cycles, and 2.5 million cycles discarded as burnin based on the convergence diagnostic. The mitochondrial genes were concatenated due to their shared history, but treated as separate partitions with distinct models. All trees were visualised with FigTree v. 1.4 (Rambaut 2009).

Detection of Conflicting Signals

We investigated the cyto-nuclear discordance and other conflicts in the phylogenetic signal with several methods. To illustrate the global reticulate signal in the data, a NeighborNet network was built in the program SplitsTree v. 4 (Kloepper and Huson 2008) with the pairwise distances calculated under the F84 correction for multiple hits. We reduced the dataset to a single best-sequenced individual per species in order to exclude the reticulations resulting from the expected recombination within species. Next, the topological disparity among individual loci was illustrated using Multi-Dimensional Scaling of pairwise Robinson-Foulds distance (Robinson and Foulds 1981) between the gene trees, as estimated by TreeSetViz v. 1.0 (Hillis et al. 2005) in Mesquite. Calculation of the RF required trimming the trees to the minimal set of 54 shared taxa from 27 species, using the R package APE (Paradis et al. 2004; R Development Core Team 2008). Finally, we investigated if topologies and branch lengths of the individual loci are consistent enough to be concatenated, by means of a hierarchical likelihood ratio test in Concaterpillar v. 1.5 (Leigh et al. 2008).

Supermatrix Phylogenetics

We created a supermatrix of the 20 nuclear and 2 mitochondrial markers in Mesquite and estimated the Maximum Likelihood (ML) phylogeny under the GTRGAMMA model in RAxML v. 7.0.4, with 1000 bootstrap replicates under the GTRCAT approximation (Stamatakis 2006). To explicitly test the likelihood of various hypotheses for Heliconiini phylogeny, several alternative topologies were created in Mesquite, representing previously identified groupings, as well as

328 suggested placements of the enigmatic genera *Cethosia*, *Laparus* and *Neruda* (Beltrán et al. 2007,
329 Brower 1994, Brower & Egan 1997, Mallet et al. 2007, Penz 1999, Penz & Peggie 2003). We then
330 re-estimated the ML tree under the GTRGAMMA model using each topology as a constraint. The
331 likelihood scores of the original and alternative trees were compared using the Shimodaira-
332 Hasegawa test (Shimodaira and Hasegawa 1989) and the Expected Likelihood Weights based on
333 1000 bootstrap replicates (Strimmer and Rambaut 2002). A separate phylogeny was generated for
334 the unpartitioned whole mitochondrial alignment in RAxML under the GTRGAMMA model with
335 1000 bootstrap replicates.

336 We estimated a calibrated Bayesian phylogeny using the program BEAST v. 1.7.5
337 (Drummond et al. 2006). In order to avoid incorrect estimates of the substitution rate parameters
338 resulting from the inclusion of multiple samples per species, this analysis was based on a pruned
339 alignment with one individual per species. The only exception is the inclusion of 3 races of *H.*
340 *melpomene* and 2 races of *H. erato*, where deep geographical divergences are found (Quek et al.
341 2010). The Vagrantini sequences were not used, as BEAST can estimate the placement of the root
342 without an outgroup (Drummond et al. 2006). Thus the analysis included 78 taxa and the
343 substitution rate models were re-estimated appropriately (Table 1). We linked the topology, but
344 modelled an uncorrelated lognormal clock and the substitution rate separately for each locus
345 (Drummond et al. 2006). Substitution rates were drawn from the overdispersed gamma distribution
346 prior with shape parameter k=0.001, scale parameter theta=1 and starting value 0.001 for nuclear
347 genes, and k=0.01 for the faster-evolving mitochondrial loci (van Velzen 2013). We used a Birth-
348 Death tree prior and empirical base frequencies to limit the computation time for the heavily
349 parametrised model. As no fossils of Heliconiini or closely related tribes are known, we used a
350 secondary calibration point from the dated phylogeny of Nymphalidae (Wahlberg et al. 2009; van
351 Velzen et al. 2013). The age of the root was modelled as normally distributed with a mean of 47 Ma
352 and a standard deviation of 3.0 Ma, corresponding to the 95% confidence intervals of the Acraeini-
353 Heliconiini split found by Wahlberg et al. (2009). Four independent instances of the MCMC chain

were ran for 100 million cycles each, sampling the posterior every 10000 cycles and discarding 10 million cycles as burnin. The input .xml file generated in BEAUti v. 1.7.5 (Drummond et al. 2010) can be found in the Online Appendix 3. To ensure that the results are driven by the data and not the priors, we executed a single empty prior run. Convergence of the continuous parameters was evaluated in Tracer v. 1.4, and the Maximum Clade Credibility tree with mean age of the nodes was generated using LogCombiner v. 1.7.5 and TreeAnalyser v. 1.7.5 (Rambaut and Drummond 2010).

Multispecies Coalescent Phylogenetics

To account for the heterogeneous phylogenetic signal resulting from gene flow, hybridisation and incomplete lineage sorting, we applied a variety of multispecies coalescent (MSC) analyses that take as input both the raw alignment and individual gene trees). We first used the established method of minimising deep coalescences (MDC) (Maddison and Knowles 2006), taking advantage of a dynamic programming implementation in the package PhyloNet (Than et al. 2008). 100 bootstrap input files containing 100 trees were drawn randomly without replacement from the distribution of Bayesian gene trees for the 21 loci, an MDC phylogeny was estimated for each input and a 50% majority rule consensus was taken.

Bayesian Concordance Analysis (BCA) is an MSC method that attempts to reconcile the genealogies of individual loci based on posterior distributions, regardless of the sources of conflict (Larget et al. 2010). BCA generates Concordance Factors (CFs), which show what proportion of loci contain a particular clade, and estimates the primary phylogenetic hypothesis from the best-supported clades. CFs offer a powerful alternative to traditional measures of support and can be conveniently estimated in the program BUCKy (Ané et al. 2007; Larget et al. 2010). We executed two runs of one million MCMC cycles in BUCKy based on the 21 posterior distributions of gene trees from MrBayes.

Another approach to the multispecies coalescent is to estimate the gene trees and the species tree simultaneously, explicitly modelling the sources of incongruence (Edwards et al. 2007). We

applied this technique using *BEAST, a program harnessing the power of BEAST and simultaneously implementing a powerful MSC algorithm that estimates the species tree and the embedded gene trees, as well as the population sizes of the lineages (Heled & Drummond 2010). Effective calculation of the population size parameters requires a thorough multilocus sampling of each species in the analysis, which forced us to reduce the dataset to species with a minimum of three individuals from at least two distinct populations (the *BEAST dataset). The final alignment included 87 terminal taxa in 17 species of *Eueides* and *Heliconius*. We re-estimated the individual substitution models for each partition, used a constant population size coalescent tree model and implemented other priors as described above for BEAST. We carried out four independent runs of 500 million cycles each, sampling every 10000 cycles, generated a maximum clade credibility species tree and visually summarised the 21 gene trees by plotting in DensiTree (Bouckaert 2010). Online Appendix 4 contains the .xml file for this analysis.

Sequence alignments and phylogenetic trees were deposited in TreeBase (http://purl.org/phylo/treebase/phylows/study/TB2:S15531).

Changes in the Diversification Rate

The formal analyses of diversification dynamics were based on the output of the Bayesian supermatrix analysis in BEAST and conducted in R. Errors in divergence time estimates are not expected to affect the divergence rate calculations significantly (Wertheim and Sanderson 2011), and the semi-log lineage through time plots (LTT) of 200 randomly selected posterior trees formed a narrow distribution around the maximum clade credibility (MCC) tree with mean node ages. Hence we based all the analyses on the MCC tree of Heliconiini with one individual per species, excluding outgroups and *Cethosia*.

We searched for the signal of change in diversification rate using TurboMEDUSA, which identifies shifts *a posteriori* through stepwise AIC (Alfaro et al. 2009). We wanted to investigate whether the Heliconiini have undergone significantly faster diversification during the periods of

406 dramatic environmental change at either 12 or 4.5 Ma, whether the diversification rate of
407 Heliconiini decreased with time due to limiting species density effects (Fordyce 2010; Etienne et al.
408 2012b), or increased as new lineages evolved novel colour patterns and drove positive mimetic
409 interactions that reduce competition (Elias et al. 2009). To compare these possibilities explicitly, we
410 fitted maximum likelihood models of increasing complexity to the MCC tree, accounting for the
411 uncertainty in the estimates of recent speciation (protracted speciation) and extinction rates (pull of
412 the present) by truncating the phylogeny to 1 Ma before present (Etienne and Haegeman 2012). The
413 following models were fitted and compared using the Akaike weights for all Heliconiini and for
414 *Heliconius* alone: pure birth, with a constant rate or with a shift in rate (PB); birth-death with and
415 without changes in rate (BD); diversity dependent model without extinction (DDL); diversity
416 dependent model with linear terms for speciation or both speciation and extinction (DDE); DDE
417 with rate shifts. We included rate shifts at an unspecified time, at 12 and 4.5 Ma, as well as at 11
418 and 3.5 Ma to account for possible delayed effects. The likelihood was conditioned on the survival
419 of phylogeny in all runs and it was assumed that there are six species missing for Heliconiini and
420 two for *Heliconius* (Lamas 2004). A possible slowdown in diversification rate after an initial rapid
421 radiation was evaluated by calculating the gamma statistic (Pybus and Harvey 2000) and its
422 significance tested in a Monte Carlo Constant Rates (MCCR) test with 1000 replicates in the
423 package LASER (Rabosky 2006).
424
425
426
427
428
429
430
431

RESULTS

Sampling and DNA Sequencing

We successfully combined three approaches to sequencing, which resulted in the high taxonomic coverage and intraspecific sampling necessary for the MSC methods, and a sufficient sampling of loci for each individual (Online Appendix 1). Most of the dataset consists of Sanger sequences from 108 individuals, 26 of which were already published in GenBank. We also obtained two classic lepidopteran markers *CoI/II* and *EF1α* from respectively 13 and 11 out of 14 historical specimens, thus adding eight species of Heliconiini that have not been sequenced previously. We did not manage to obtain any data from *Philaethria andrei*, *P. browni*, *P. romeroi*, *Eueides emsleyi*, *E. libitina*, *Heliconius lalitae* or *H. metis* (Lamas 2004; Constantino and Salazar 2010; Moreira and Mielke 2010).

We capitalised on the availability of Illumina data by generating *de novo* assembly contigs for further 57 individuals. The N50 of the Abyss assemblies ranged from 552 to 1921 bp (average 1206) and all the nuclear markers were successfully recovered by megaBLAST from every assembly. Whole mitochondrial sequences of the same individuals were recovered by read mapping, with about a 400 bp stretch of the hypervariable control region (Heliconius Genome Consortium 2012) incomplete in some sequences. We obtained a depth of coverage over 100x and high confidence in the base calls due to the high copy number of mtDNA in the tissue. Finally, we included the sequences extracted from the *Heliconius melpomene* genome, as well as the previously published mitochondrial sequence of *Acraea issoria* (Heliconius Genome Consortium 2012).

The sequence data for 20 nuclear and 2 mitochondrial genes encompass 71 out of 78 (91%) of the officially recognised species of Heliconiini, including 44 out of 46 species from the focal genus *Heliconius* (Lamas et al. 2004; Beltrán et al. 2007; Mallet et al. 2007; Constantino and Salazar 2010). Although the taxonomic validity of some species is contested, we found that the diversification analysis is robust to altering the number of missing species. Some recognised taxa

diverged very recently, as shown by the BEAST chronogram (Fig. 1) in case of the *Philaethria diatonica*/*P. neildi*/*P. ostara* complex and the *Heliconius heurippa*/*H. tristero* pair, the latter of which could be considered races of *H. timareta* (Nadeau et al. 2013). However, the exact relationship between genetic differentiation and taxonomic species identity in the highly variable, mimetic Heliconiini remains unclear (e.g. Mérot et al. 2013). Importantly, 36 species are represented by multiple individuals, usually from distant populations, allowing for more accurate estimation of sequence evolution rates, and detection of species paraphyly. The number of individuals represented by each marker ranges from 40% for *Hcl* to 98% for *CoI/II*, and only four specimens are represented exclusively by mitochondrial DNA (Online Appendix 1).

Pervasive Conflict Between the Loci

Our nuclear markers span 11 out of 21 chromosomes (Table 1; Heliconius Genome Consortium, 2012) and have both autosomal and sex chromosome Z-linked inheritance. We examined the conflict between individual markers in the entire tribe and in the genus *Heliconius* alone, using both gene tree summary methods and approaches utilising the raw sequence alignments. The maximum likelihood analysis of the core matrix in Concaterpillar rejected concatenation of any of the loci due to significant differences in both topology and substitution rate of individual partitions, but the exact nature of the discordance is unclear. A Multi-Dimensional Scaling ordination of pairwise RF distances between the gene trees does not reveal clustering by chromosome and the separation between many nuclear loci appears much greater than between nuclear and mitochondrial trees (Fig. 2). Consistent with this is the fact that the whole mitochondrial phylogeny of select taxa (Fig. 3) shows few differences from the tree based on the mixed marker supermatrix (Fig. 1), highlighting that cyto-nuclear discordance is not the primary source of incongruence in the dataset.

The coalescent approaches reveal the high extent of marker conflict in the *Heliconius* data. Gene tree topologies from the explicit Bayesian modelling of incomplete lineage sorting (ILS) in

*BEAST are highly varied, with a particularly high degree of reticulation in the *H. melpomene*/*cydno* and the *H. hecale* (silvaniform) clades, where extensive horizontal gene flow has been observed previously (Sup. Fig. S1; Brown 1981; Martin et al. 2013). Another Bayesian method, BUCKy, infers the species in the presence of marker incongruence without modelling specific reasons for the observed discordance and calculates the Bayesian concordance factors that illustrate the proportion of partitions in the dataset that support a particular grouping (Ané et al. 2007; Baum 2007; Larget et al. 2010). The concordance of the loci for *Heliconius* is strikingly low (Fig. 4), although the topology is consistent with the results of other analyses (Fig. 1 and 3, Sup. Fig. S2-S6).

Further strong evidence of widespread incongruence comes from the NeighborNet network characterised by a high delta score of 0.276, which shows that the structure of the data is not entirely tree-like (Sup. Fig. S3). This can be partially attributed to the effect of missing data, yet even a fit based on the 30 species with little missing data produced a delta score of 0.11, proving a substantial amount of non-bifurcating signal across the tribe (Holland et al. 2002). The most noticeable reticulations are found between nodes linking genera and the major clades of *Heliconius*, possibly due to pervasive gene flow during the diversification of the main extant lineages (Sup. Fig. S3).

Topological Consistency Across Optimality Criteria

Although no trees are identical, the results from our Bayesian, Maximum Likelihood and distance-based network analyses of the supermatrix are very similar (Fig. 1, Sup. Fig. S3, S4). Two nodes stand out as unstable. *Cethosia* is variably placed as a sister taxon to either Acraeini (MP, ML, NeighborNet) or Heliconiini (Bayesian), despite the reasonably extensive sampling of 11 loci for *C. cyane*, while the position of *Podotricha* in relation to *Dryas* and *Dryadula* varies between all analyses. Most problematic are relations among the species within *Eueides*, where the position of four out of 10 taxa cannot be resolved with good support. The poor resolution for both *Eueides* and

Podotricha can probably be attributed to insufficient site coverage, which produces high uncertainty due to patchily distributed missing data (Wiens and Morrill 2011; Roure et al. 2013). We re-estimated the relations of *Eueides* based solely on a core set of 11 genes with coverage for at least 7/10 species and recovered a much better supported tree (Sup.. Fig. S6). We recommend studies focusing on *Eueides* use this specific phylogeny, but the exact relations of *E. procula*, *E. lineata* and *E. heliconioides* remain unclear.

Although our Bayesian maximum clade credibility tree is largely consistent with the topology estimated by Beltrán *et al.* (2007), significantly increasing the dataset from 113 to 180 individuals and five to 21 loci allowed us to resolve many critical nodes. The major differences are in the relations of the basal genera, which we infer to form a well-supported grade, with *Eueides* as the definitive sister genus of *Heliconius* (Fig. 1). Importantly, we confirm that the enigmatic genera *Laparus* and *Neruda* are nested within *Heliconius*, as further supported by ELW and SH tests (Table 2), although *Neruda* is closer to the base of the genus than previously estimated. We find that the other so called "primitive" (Brown 1981) clade of *Heliconius* consists of two separate groups, which are by no means basal to the other taxa, raising questions about the apparently unequal rate of morphological evolution in the genus.

The maximum likelihood tree is similar to the Bayesian phylogeny, although characterised by lower overall support, especially for the nodes linking the genera and subgenera (Sup. Fig. S4). The nodes differing between the two trees are also the nodes that cannot be unequivocally confirmed by either the SH and the ELW test (Table 2). For instance, the highest posterior probability in the ELW test (0.21) is given to a tree placing *H. heurippa* as a sister species to *H. timareta*, a result recovered in both the Bayesian analysis and a recent genome-wide study (Nadeau et al. 2013). Thus we suggest that the Bayesian tree should be preferred as a more accurate picture of the phylogenetic relationships, although the ML tree based on the complete dataset is still useful to uncover multiple polyphyletic species. Notably, *H. luciana* is nested within *H. elevatus,* and *H. wallacei i*s polyphyletic with respect to *H. astraea*. These results must be interpreted with caution,

as the inference relies on poorly covered museum specimens and may be sensitive to long branch attraction (Wiens and Morrill 2011).

Our whole mitochondrial phylogeny is largely consistent with the results of the multilocus supermatrix analysis and well-supported for 46/57 nodes (Fig. 3), despite the relatively limited taxonomic coverage of only 29 Heliconiini for which short-read data was available. In contrast to the multilocus dataset, mitochondrial genomes are not very useful for resolving relationships between major clades within *Heliconius*, as the position of *Neruda*, *xanthocles* and *wallacei* clades is poorly supported. An important deviation from the predominantly nuclear multilocus phylogeny is the placement of *H. pachinus* as a sister taxon of *H. timareta*, rather than *H. cydno*. This may reflect the overall instability resulting from a high extent of reticulation in the *melpomene*/*cydno*/*timareta* assemblage (Heliconius Genome Consortium 2012, Martin et al. 2013, Mérot et al. 2013). Furthermore, we find a surprising positioning of *H. hermathena* within *H. erato* (Jiggins et al. 2008), which is also not supported by any of the analyses of the 21 locus matrix. The mitochondrial tree confirms previous observations of deep biogeographical splits in the widespread, highly diversified *H. erato* and its co-mimic *H. melpomene* (Brower 1994a). Within *H. melpomene* we find a well-supported distinction between races found to the West and East of the Andes, although our data place the individuals from French Guiana with the specimens from the Western clade, in contrast to a whole-genome phylogeny (Nadeau et al. 2013) (Fig. 1). *H. erato* shows the opposite pattern in both mitochondrial and nuclear data, whereby the Guianian races form a fully supported clade in the monophyletic group of taxa from East of the Andes.

The variety of multi-species coalescent (MSC) methods that we applied brings a new perspective to the phylogenetic signals in the Heliconiini. Notably, different approaches and combinations of the data yield highly consistent topologies, although the support for the individual nodes varies. We used three techniques that attempt to deal with various aspects of the observed incongruence between loci. The maximum parsimony approach of MDC is a summary method deriving a species tree from the distribution of gene trees with single or multiple terminals per

562 species, intended to address the effects of ILS (Maddison 1997; Maddison and Knowles 2006).
563 Although infrequently considered in recent studies, MDC has been implemented in multiple
564 packages (Maddison and Maddison 2011; Than et al. 2008) and offers superior speed of analysis
565 when compared to other MSC techniques. In case of our complete dataset, a run with 100 bootstrap
566 datasets took a few minutes. The resulting topology is nonetheless very different from the other
567 results, showing a number of unexpected and poorly supported groupings. The lumping of all non-
568 *Heliconius* genera, and the monophyletic *Neruda*/*xanthocles*/*wallacei* clade stand out in contrast to
569 other proposed trees (Sup. Fig. S6). Interestingly, many of the relations that are poorly supported in
570 the supermatrix phylogenies are also not resolved in the consensus MDC tree, showing that MDC is
571 highly conservative with regard to the placement of taxa unstable in individual gene trees.
572 The Bayesian MSC approach implemented in *BEAST uses MCMC to co-estimate the
573 species-level tree and the contained gene trees by estimating demographic parameters together with
574 the phylogeny, but only with an appropriate intraspecific sampling (Heled and Drummond 2010).
575 Although computationally intensive, *BEAST models ILS and proposes a species tree without
576 ignoring the underlying heterogeneity in specific locus genealogies, performing exceptionally well
577 even with the most difficult cases combining large population size with short divergence times
578 (Leaché & Rannala 2010). We analysed the small dataset of the 17 best-sampled species and
579 recovered a tree which agrees with the supermatrix analyses (Sup. Fig. S2), except for the position
580 of *Neruda aoede*, which was placed as a sister taxon to the *H. xanthocles*/*L. doris* clade with
581 relatively low posterior probability. Furthermore, the mean ages of nodes are nearly identical to
582 those proposed in a supermatrix analysis, with similar 95% confidence intervals. Although the
583 species tree is largely as predicted, we observe high levels of incongruence in the underlying
584 distribution of gene trees (Sup. Fig. S1). Differences in the depth of coalescence are clear
585 throughout the tree and reticulation is again especially apparent in the *H. melpomene/cydno* clade.
586 The estimated population size values are also consistent with a previous comparison based on two
587 nuclear loci, showing a higher population size of *H. erato* (1.33×10^6 individuals) when compared to

588 *H. melpomene* (1.02×10^6) (Flanagan et al. 2004).

589 While *BEAST is a powerful approach to account for ILS under a complex evolutionary
590 model, it does not take into account various other sources of data heterogeneity. BUCKy derives a
591 topology together with CFs, which represent the proportion of the genome supporting a particular
592 clade. The most likely clade may therefore receive low support if it is represented in only a few of
593 the Bayesian gene tree posteriors (Larget et al. 2010). The method is thus able to propose a robust
594 topology in the face of ILS, hybridisation or other complex processes. As described above, we find
595 the phylogeny derived by BUCKY to be entirely consistent with the Bayesian analysis of
596 concatenated sequence, although the recovered CFs are much lower than any other measure of
597 support applied to our data. Importantly, most of the nodes connecting the major clades in the tree
598 have CFs below 0.5, with the notable exception of the silvaniform/*melpomene* split (Fig. 4). The
599 same nodes correspond to the reticulations in the NeighborNet analysis (Sup. Fig. S3), cases of low
600 support in the MDC tree and its disagreement with the supermatrix analysis (Sup. Fig. S6), nodes
601 that cannot be rejected in the ML tests of topologies (Table 2), and the uncertain nodes in the whole
602 mitochondrial tree (Fig. 3).

603

604 *Tempo of Diversification*

605 The phylogeny estimated under a relaxed clock model in BEAST shows diversification
606 dynamics that differ from previous estimates, with the splits between the genera of Heliconiini
607 being older and the extant species and subgenera much younger than previously thought (Table
608 3)(Mallet et al. 2007). The most speciose genera *Heliconius* and *Eueides* separated 17 Ma and both
609 started to diversify around 10 Ma, and the six major clades of *Heliconius* (corresponding to *H.*
610 *erato*, *H. sara*, *H. xanthocles*, *H. wallacei*, *H. melpomene*/silvaniforms and *Neruda*) all started to
611 diversify between 5 and 4 Ma (Fig. 1). The lineage through time plot (LTT) for Heliconiini suggests
612 a period of stasis corresponding to the mid-Miocene 16-11 Ma (Hoorn et al. 2010), and followed by
613 a sudden increase in the number of extant lineages (Fig. 5a). In case of the 45 *Heliconius* species, a

shorter slowdown is found between 7 and 4.5 Ma (Fig. 5b) (Hoorn et al. 2010). As expected from the LTT plots, the MCCR test detects no evidence for an overall slowdown in the diversification rate (Heliconiini: gamma= 2.643, *p*=0.996; *Heliconius*: gamma= 0.153, *p*=0.617).

Maximum Likelihood (ML) modelling strongly supports the Birth-Death model with rate shift as the best fit for Heliconiini (Akaike weight of 0.92; Table 4). Both DDD and turboMEDUSA models demonstrate that around 11 Ma the speciation rate of Heliconiini increased dramatically from 0.19 to 0.40 new species per lineage per million years, and the shift was accompanied by an increase in the turnover rate from 0.11 to 0.65. The results for *Heliconius* are less clear, as equal Akaike weights (0.30) are given to the Pure Birth models without rate changes, and with an almost twofold increase in speciation rate 4.5 Ma (Table 4). TurboMEDUSA and DDD models allowing for a shift at an unspecified time also find that speciation accelerated 10-11 Ma and 4-5 Ma.

640 DISCUSSION

641

642 *Stable Topology Despite Marker Incongruence*

643 We approached the problem of phylogeny reconstruction in a difficult mimetic assemblage
644 through extensive intraspecific sampling of 22 markers from nearly all species in the clade, and
645 compared the results between multiple philosophically distinct analytical approaches. As next
646 generation sequencing technologies become widely accessible and the average number of loci used
647 in systematic studies increases rapidly, Multi-Species Coalescent (MSC) methods gain in
648 importance as means of detecting and accounting for incongruence in multilocus data (e.g. Lee et al.
649 2012; Barker et al. 2013; Smith et al. 2013). However, their relative merits and utility at different
650 levels remains contested (Song et al. 2012; Gatesy and Springer 2013; Reid et al. 2013). The
651 systematic relations of the tribe Heliconiini, which diverged from its extant outgroup about 47 Ma,
652 can be effectively resolved with both MSC and supermatrix approaches, yielding highly similar
653 topologies across a range of different sub-sampling schemes that correspond to the requirements of
654 individual algorithms (Fig. 1, 3 and 4; Sup. Fig. S2-S6). Nonetheless, consistent with the recent
655 radiation of the group, large effective population sizes and known hybridisation between many
656 species, we observed high heterogeneity among sampled fragments of the genome that differ
657 markedly in both topology (Fig. 2, Sup. Fig. S1) and rates of evolution (Concaterpillar analysis).
658 Such heterogeneity might have been expected to pose a significant challenge for the concatenation
659 methods (Degnan and Rosenberg 2006; Edwards et al. 2007; Edwards 2009; Knowles and Kubatko
660 2010; Leaché and Rannala 2010). However, the only method producing an obviously different
661 phylogeny is Minimising Deep Coalescences (MDC; Sup. Fig. S6), which fails to resolve 34 out of
662 62 nodes in the tree with bootstrap support above 0.9, and is the only method to suggest monophyly
663 of *Eueides* with other basal genera of Heliconiini. MDC derives a species tree from point estimates
664 of gene trees and can be expected to perform poorly with a relatively limited number of gene trees
665 that are not always fully resolved, leading to a complete polytomy in some of the clades (Gatesy
666 and Springer 2013). However, the MDC result is an indicator of instability, as well-resolved and

667 consistent gene trees should produce a good quality MDC tree.

668 Recent studies have proposed that likelihood-based MSC techniques perform better than and
669 should be preferred to integration over individual gene trees, due to their potential to capture
670 synergistic effects between partitions (Leaché and Rannala 2010; Reid et al. 2013), mirroring the
671 phenomenon of hidden support found when multiple markers are concatenated (Gatesy and Baker
672 2005). Our results support this observation and further show that high degrees of conflict between
673 many partitions can be reconciled by both supermatrix and MSC approaches to extract the
674 predominant signal of speciation. The superiority of the MSC methods lies in the effective
675 demonstration of incongruences, represented by lower support values or concordance factors
676 assigned to the more difficult nodes (Belfiore et al. 2008). The Bayesian concordance analysis in
677 BUCKy assigns insignificant concordance factors to most of the nodes separating major subgenera
678 of *Heliconius*. Two of these nodes (*H. wallacei* and *N. aoede*; Fig. 4) are also only weakly
679 supported by the *BEAST coalescent model, and correspond to the areas of high reticulation in the
680 NeighborNet network, reflecting conflicting signals (Sup. Fig. S3). The same nodes are all assigned
681 a posterior probability of one in the Bayesian supermatrix analysis (Fig. 1), potentially leading to
682 the erroneous conclusion that all the data point unequivocally to the inferred relations.

683 Our study highlights an important practical consideration in choosing the optimal analytical
684 approach, where the requirements of the selected algorithm have to be reconciled with a realistic
685 sampling of taxa. Our final goal of testing hypotheses regarding the diversification dynamics of
686 Heliconiini can be met only if the number of included taxa is maximised. Despite a substantial
687 effort we only managed to secure single samples of the rare or geographically restricted species, and
688 some of them are represented solely by historical specimens with limited potential to generate
689 extensive multilocus data. Considering that our study group is intensively studied and exceptionally
690 well represented in research, museum and private collections due to its aesthetic appeal (Mallet et
691 al. 2007), it would be considerably more challenging to obtain a complete sampling of many other
692 groups. Another difficulty stems from the fact that the advanced coalescent techniques like BUCKy

693 and *BEAST perform best with multiple samples per species, which should capture intraspecific
694 diversity (Heled & Drummond 2010, Reid et al. 2013). Finally, much of the uncertainty in the
695 estimates can be attributed to missing data, which can negatively affect the estimation of both
696 individual gene trees and the encompassing species tree (Wiens and Morrill 2011; Roure et al.
697 2013). When fitting a NeighborNet network, we found that although the percentage of data missing
698 from the matrix does not explain all of the observed reticulation and the high delta score, it causes
699 these parameters to increase, thus suggesting that the data completeness at each alignment position
700 must be maximised to identify genuine incongruence. We observe that in many cases of biological
701 interest it will be a formidable challenge to generate the ideal dataset that (i) has little missing data,
702 (ii) comprises a large, genome-wide sample of loci, (iii) includes all taxa, and (iv) captures
703 intraspecific variability. In case of Heliconiini, the supermatrix approach based on a limited number
704 of markers (22) helped us to maximise taxonomic inclusiveness without compromising our ability
705 to reconstruct a phylogeny in the light of conflicting biological signals.
706
707 *Divergence time estimates*
708 Our phylogeny of Heliconiini brings novel insight into the diversification dynamics of the
709 clade. Although most age estimates for *Heliconius* agree with other studies, the deeper nodes are
710 older than previously suggested (Table 3). There is little agreement on the dates above the species
711 level, and the studies to date either suffer from insufficient taxon sampling (Pohl et al. 2009,
712 Wahlberg et al. 2009, Cuthill and Charleston 2012; Table 3), or use markers unlikely to be
713 informative above a relatively low level of divergence (Mallet et al. 2007). For instance, the mean
714 age of the split between *Heliconius* and *Agraulis* is estimated as 32 Ma in the study of Pohl et al.
715 (2009), which includes only 3 species of Heliconiini; 26.5 Ma in Wahlberg et al. (2009), including
716 one species per genus; or 21 Ma in the present study (Fig. 1; Table 3). Conversely, Mallet et al.
717 (2007) find the divergences between the basal genera of Heliconiini to be much younger than we
718 propose, likely due to an effect of using a fast-evolving mitochondrial locus without partitioning

719 (Brandley et al. 2011).

720 Our own ability to correctly falsify the hypotheses regarding the diversification of
721 Heliconiini hinges on having a nearly complete phylogeny, yet none of our MSC analyses consider
722 as many species of Heliconiini as the Bayesian supermatrix estimate. We are confident that the
723 values proposed by the supermatrix method can be trusted, as both the topology and the branch
724 lengths are consistent with the results inferred by *BEAST based on a smaller dataset (Table 3;
725 Sup. Fig. S2). We find that the ages of the deeper nodes and the length of terminal branches are not
726 inflated by the supermatrix method in comparison to *BEAST, contrary to the predictions from
727 simulations (Burbrink and Pyron 2011), and both methods infer similar mean age for the observed
728 splits, for instance 10.5 Ma for the basal divergence of *Heliconius* into the *H. erato* and *H.*
729 *melpomene* lineages, or 2-3 Ma for the diversification of *H. melpomene* and silvaniform clades.
730 Hence we offer a new perspective on the dating of Heliconiini radiation with a nearly complete set
731 of divergence time estimates based on a well-resolved and supported tree.

732

733

734 *Rapid Adaptive Radiation of* Heliconius

735 *Heliconius* have undergone a rapid adaptive radiation *sensu* Schluter (2000), associated with
736 the evolution of Müllerian mimicry, close coevolution with the Passifloraceae host plants (Benson
737 et al. 1975) and other traits unique among the Lepidoptera (reviewed by Beltrán et al. 2007).
738 Maximum Likelihood models demonstrate that around 11 Ma the speciation rate of Heliconiini
739 increased dramatically from 0.19 to 0.40 new species per lineage per million years, and the shift
740 was accompanied by an increase in the turnover rate from 0.11 to 0.65, indicating higher likelihood
741 of extinction of the lineages. Our results are consistent with the radiation having been stimulated by
742 environmental factors such as mountain uplift, and creation of elevation gradients facilitating
743 parapatric speciation (Wesselingh et al. 2009, Hoorn et al. 2010, Turchetto-Zolet et al. 2013).
744 Consistent with the inference of the Central and Eastern Andean slopes as the “species pump” of

745 Heliconiini (Rosser et al. 2012), we find that diversification of *Heliconius* and *Eueides* into
746 subgeneric clades occurred within the two million years after the major Andean uplift event 12 Ma,
747 and that the modern species of *Heliconius* started to diversify after the last intensive orogenic event
748 4.5 Ma (Gregory-Wodzicki 2000). Contrary to our expectations, mimicry does not leave a clear
749 signature of positive feedback on the rate of diversification. Although mimetic interactions have
750 been repeatedly invoked as drivers of speciation in Heliconiini and butterflies generally (Bates
751 1862; McMillan et al. 1997; Mallet and Joron 1999; Elias et al. 2008; Jiggins 2008; Savage and
752 Mullen 2009) and mimicry can possibly decrease the risk of extinction as a consequence of reduced
753 predation rates (Vamosi 2005), model fitting does not support an exponential increase in rates of
754 speciation.

755 Although we find sudden increases in speciation rates, there is no indication that the rates
756 slowed down significantly afterwards. This result is consistent with a recent critique (Day et al.
757 2013) of the traditional prediction that large radiations should display a pattern of an initially high
758 net diversification rate, decreasing as the ecological niches fill up (e.g. Rabosky and Lovette 2008).
759 This expectation is reasonable for spatially limited island radiations that constitute the majority of
760 study cases to-date, but it does not necessarily apply to continental radiations in the tropics, where
761 the scale and complexity of the ecosystems are likely to generate a number of suitable niches
762 greatly exceeding even the cladogenetic potential of large radiations (Day et al. 2013). So far,
763 steady diversification of a widely distributed taxon has been demonstrated in the African *Synodontis*
764 catfish (Day et al. 2013) and the Neotropical Furnariidae ovenbirds (Derryberry et al. 2011), but the
765 generality of this pattern remains unknown. Heliconiini constitute an interesting case of a
766 widespread, continental radiation where at least one sharp transition to a higher species turnover
767 punctuates an otherwise steady diversification. Thus the physical environment has acted a driver of
768 diversification, but did not limit cladogenesis.

769 Some uncertainty surrounds the last few million years of evolution of Heliconiini. Early
770 speculation regarding the drivers of speciation suggested diversification in allopatry, as the

771 rainforest habitat occupied by most species in the group has undergone cycles of contraction and
772 expansion in response to recent climatic variation (Turner 1965; Brown et al. 1974; Brown 1981;
773 Sheppard et al. 1985; Brower 1994a). The hypothesis of vicariant cladogenesis has been
774 subsequently criticised due to a lack of evidence for forest fragmentation in pollen core data
775 (Colinvaux et al. 2000, Dasmahapatra et al. 2010), as well as the likelihood of parapatric speciation
776 (Mallet et al. 1998). The decrease in observed diversification over the last million years is likely due
777 to our limited ability to delineate species in the assemblages of highly variable taxa like *Heliconius*
778 – a phenomenon that has been termed "protracted speciation" (Etienne & Haegemann 2012). We
779 provide direct evidence that most specific divergences between species of Heliconiini occurred
780 during the Miocene, and that both climate and orogeny strongly influenced the pattern of
781 diversification, although we cannot directly test the causes of this association with these data.
782
783 *Taxonomic and Systematic Implications*
784 Application of novel algorithms to the Heliconiini data reveals a relatively stable topology
785 despite limited support. We uphold the previous re-classification of the species in the genera
786 *Neruda* (Huebner 1813) and *Laparus* (Linnaeus 1771) as *Heliconius* based on their nested position
787 (Beltrán et al. 2007). This placement is at odds with morphological evidence from adult and larval
788 characters, which puts *Neruda* and *Laparus* together with *Eueides* (Penz 1999), suggesting
789 convergent evolution of homoplasious morphological characters. Nevertheless, the molecular
790 evidence is decisive and we thus synonymize *Laparus* **syn. nov.** and *Neruda* **syn. nov.** with
791 *Heliconius*.
792 The position of the enigmatic genus *Cethosia* remains unresolved, as it currently depends on
793 the chosen method of analysis, and is unlikely to be established without a broad sampling of species
794 using multiple markers. *Cethosia* has been variably considered to be either the only Old World
795 representative of Heliconiini (Brown 1981; Penz and Peggie 2003; Beltrán et al. 2007), a genus of
796 Acraeini (Penz 1999; Wahlberg et al. 2009), or possibly a distinct tribe (Müller and Beheregaray

2010). Establishing the systematic relations between Acraeini, *Cethosia* and Heliconiini is important for the study of Heliconiini macroevolution, as it could shed light on the origins of the heliconian affinity for the Passifloraceae host plants. Known records indicate that *Cethosia* species feed on *Adenia* and *Passiflora* (Müller and Behergaray 2010), raising the possibility that Heliconiini may have evolved from an Australasian ancestor that already exhibited the modern dietary preference.

Heliconiini have been at the centre of the debate about species concepts and designation criteria, providing empirical evidence for the permeability of species barriers (Mallet et al. 2007, Nadeau et al. 2012, Martin et al. 2013). At the same time, new species continue to be described based on morphological, genetic or karyotypic evidence (Lamas et al. 2004; Constantino and Salazar 2010; Dasmahapatra et al. 2010; Moreira and Mielke 2010), although the validity of the taxonomic status of some of these new lineages is disputed (J. Mallet and A. Brower, *pers. comm*.). Our diversification analysis is therefore prone to error resulting from the uncertainty in the number of terminal taxa that should be considered. We assume the number of species in the clade to be 78, reflecting the published taxonomy (Lamas 2004; Constantino and Salazar 2010; Rosser et al. 2012), and we deliberately exclude a formally undescribed species of *Agraulis*. Although we included *H. tristero* at the time of our analysis, it is not considered a species any longer (Mérot et al. 2013). In addition, a recent study suggests that Philaethria *pygmalion* and *Philaethria wernickei* may in fact constitute a single species (Barão et al. 2014). Although the number of Heliconiini species may therefore vary between 73 and 79, changing the number of missing species in the diversification analyses does not alter the results substantially.

Conclusion

We present a taxonomically comprehensive phylogeny of a large continental radiation characterised by extensive hybridisation, adaptive introgression and rapid speciation, and emerging as a prominent system for comparative genomics. The tribe Heliconiini has radiated in association

with environmental change in the Neotropics over the past 23 Ma and that speciation and species turnover increased dramatically at the end of the Mid-Miocene. Although there is a clear signature of processes leading to incongruence of individual gene trees and the species tree, we consistently recover the same topology using different analytical approaches. We conclude that the established supermatrix methods perform well, but are less effective in detecting the underlying conflict and estimating nodal support than the alternative Multispecies Coalescent techniques.

Müllerian mimicry affects the mode of speciation in *Heliconius*, and probably plays a role for the other, less researched genera of Heliconiini as well. Parapatry and sympatry are likely of importance in the ecological speciation of the butterflies, due to the dual role of wing patterns as both aposematic warnings under strong selection and essential cues for mating (Jiggins et al. 2001, Merrill et al. 2012). As incipient species diverge in their patterns by co-evolving with differently patterned co-mimics from multiple sympatric mimicry rings, assortative mating can lead to further genetic isolation of the lineages, enabling further divergence (Merrill et al. 2012). Conversely, the adaptive value of locally advantageous patterns facilitates adaptive introgression of pattern loci between species (Mallet et al 2007, Heliconius Genome Consortium 2012, Martin et al. 2013). Mimicry is thus an important factor in enhancing gene flow between species of *Heliconius* and *Eueides*, likely contributing to the observed levels of discordance between sampled markers. The seemingly unusual aspects of our study system, including introgression, hybridisation and speciation in sympatry, have all been only recently recognised as important evolutionary processes. We expect that reticulate signals in phylogenetic data will be increasingly important in future systematic studies and the Heliconiini represents a case study where the knowledge of specific microevolutionary processes can inform our understanding of cladogenesis at deeper timescales.

Author contributions

Designed the study : KMK, NW and CDJ. Carried out the experiments, analysed the data and drafted the manuscript: KMK. Contributed novel materials and reagents: CDJ, JM, KD, NW and AN. All authors have read and approved the final version of the manuscript.

Funding

KMK is funded by the Herchel Smith Trust, Emmanuel College and the Balfour Studentship from the Department of Zoology, Cambridge University. CDJ was supported by the Leverhulme Trust Leadership Grant. NW acknowledges funding from Kone Foundation. JM and KKD were funded through the BBSRC grant BB/G006903/1.

The authors declare no conflict of interest.

Acknowledgments

Computational analyses were performed on the RAM—bio server at the School of Life Sciences, University of Cambridge, with extensive support from Jenny Barna. We are grateful to Brian Counterman, Laura Ferguson, Marcus Kronforst, Owen McMillan and Gilson Moreira for the permission to use unpublished Illumina data. We appreciate the specimens shared by Christian Brévignon, Luis Constantino, Frank Jiggins, Mathieu Joron and the curators at Harvard Museum of Comparative Zoology, McGuire Centre, Natural History Museum London and Naturhistoriches Museum Wien. We thank Nick Mundy for the permission to use vertebrate laboratory facilities. Jessica Leigh offered help with Concaterpillar. Rampal Etienne and Carlos Peña advised us on the diversification analysis. Members of the Butterfly Genetics Group, Rob Asher, Andrew Brower, Matthieu Joron, Nick Mundy, Albert Phillimore and Neil Rosser provided helpful comments on the results.

877 FIGURES

878

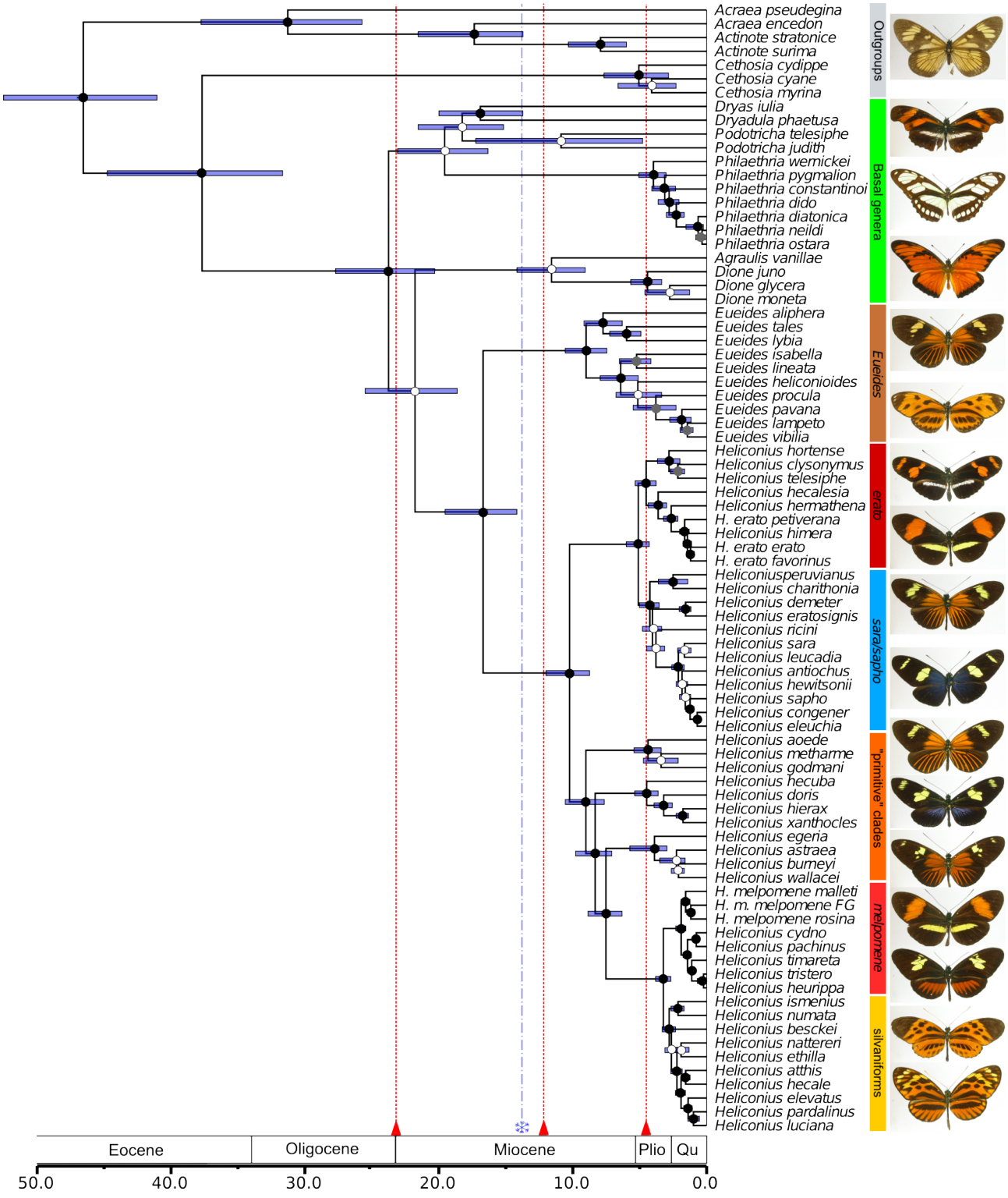

879

880 Figure 1. Bayesian phylogeny of 71 out of 78 butterflies in the tribe Heliconiini with outgroups,

881 estimated using 22 markers with an uncorrelated molecular clock method (BEAST). The age of the

882 root is calibrated based on the results of Wahlberg et al. (2009) and the bars signify the 95%

confidence intervals around the mean node ages. The dots indicate the Bayesian posterior probability of the splits: >99% (black), 95-99% (grey), <95% (white). Scale axis in Ma. Red triangles indicate the periods of Andean orogenesis 23, 12 and 4.5 Ma and the blue asterisk marks the end of the Mid-Miocene Global Optimum (Hoorn et al. 2010). Deep splits are shown within the well-studied *Heliconius erato* and *H. melpomene*. FG=French Guiana. Heliconiini exhibit complex patterns of divergence and convergence in aposematic wing patterns, top to bottom: *Actinote latior* (outgroup), *Eueides tales michaeli*, *E. lampeto lampeto*, *H. telesiphe telesiphe*, *H. erato favorinus*, *H. demeter ucayalensis*, *H. sara*, *H. aoede*, *H. doris* (blue morph), *H. burneyi jamesi*, *H. melpomene amaryllis*, *H. timareta ssp.*, *H. numata lyrcaeus*, *H. pardalinus dilatus*.

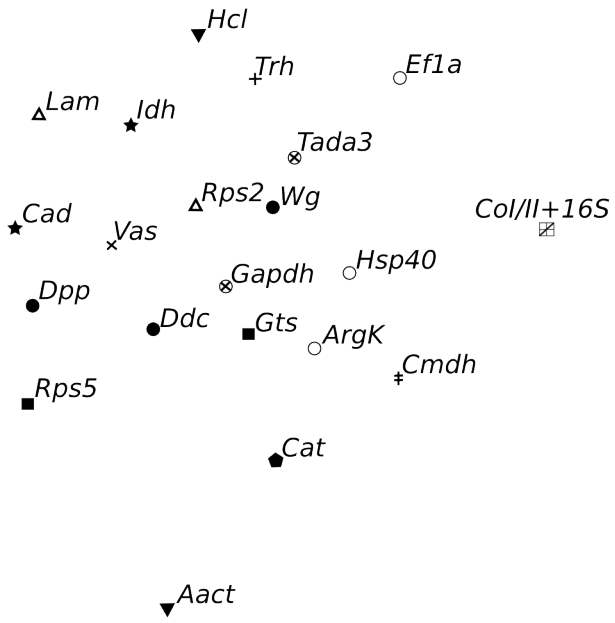

Figure 2. Multi-dimensional scaling ordination of pairwise Robinson-Foulds distances between 21 gene trees fitted in the Tree Set Visualiser shows no clear patterns of incongruence between the markers. Phylogenies of two mitochondrial and 20 nuclear markers were estimated in MrBayes. The axes have no units.

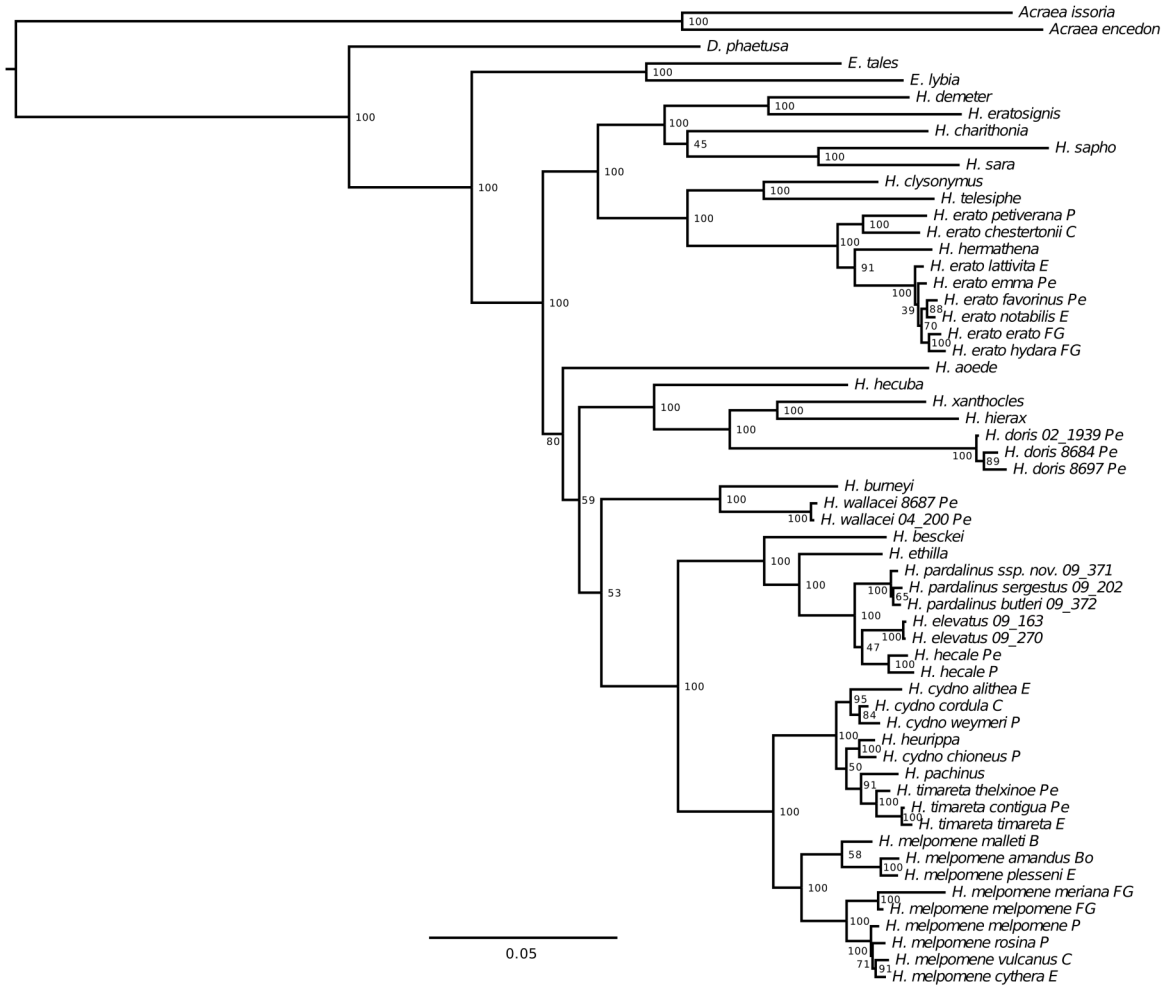

916

917 Figure 3. Whole mitochondrial maximum likelihood (RAxML) phylogeny of the genus *Heliconius.*

918 Bootstrap support values indicated. Scale bar in units of substitution per site per million years.

919 B=Brazil, Bo=Bolivia, C=Colombia, E=Ecuador, FG=French Guiana, P=Panama, Pe=Peru.

920

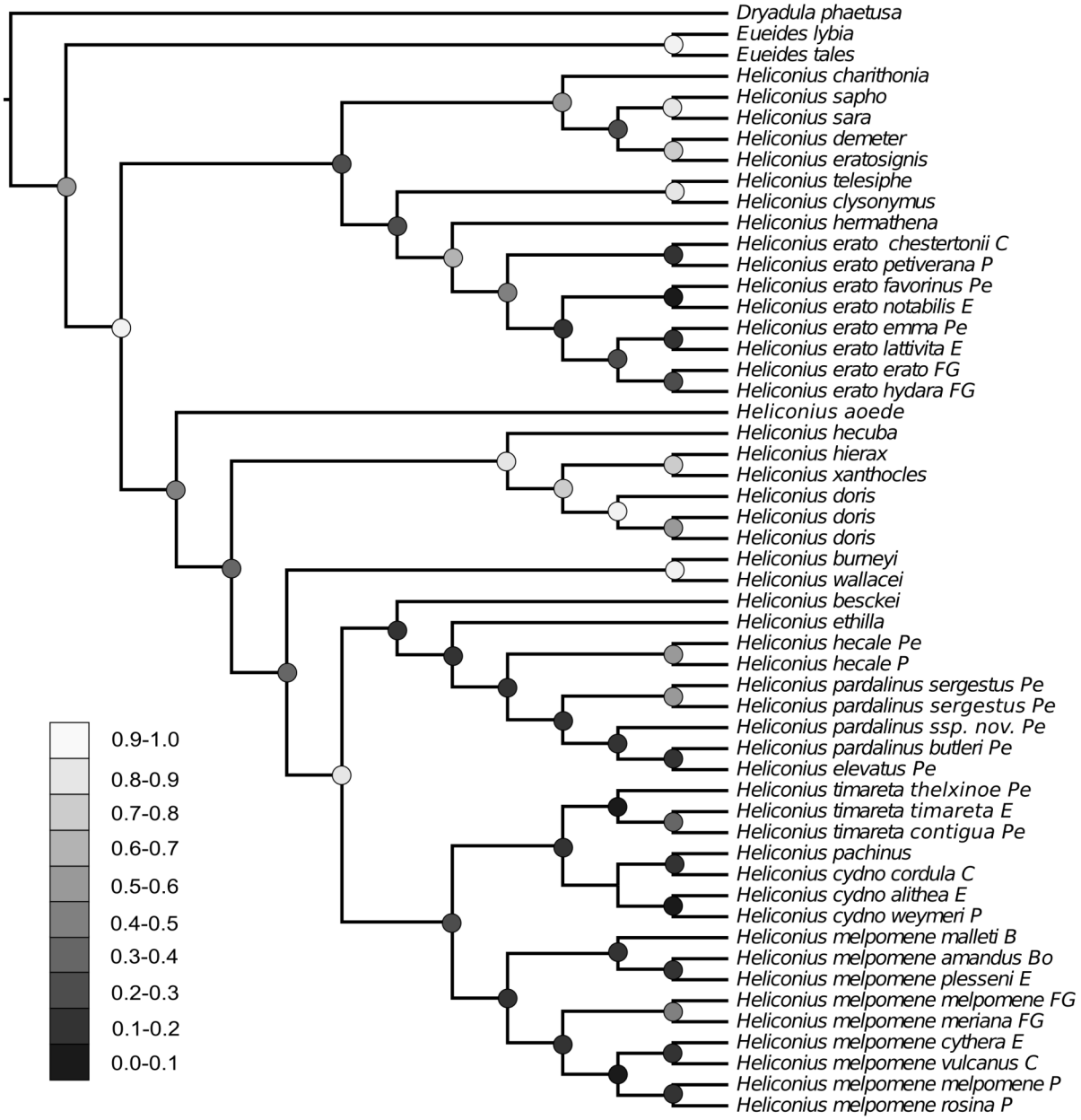

921

922 Figure 4. A phylogenetic hypothesis for *Heliconius* showing the extent of concordance between tree
923 topologies of the 21 loci estimated by Bayesian concordance analysis in BUCKy. Dots indicate the
924 Concordance Factor values for the nodes, with darker shades of grey corresponding to lower
925 support values. B=Brazil, Bo=Bolivia, C=Colombia, E=Ecuador, FG=French Guiana, P=Panama,
926 Pe=Peru.

927

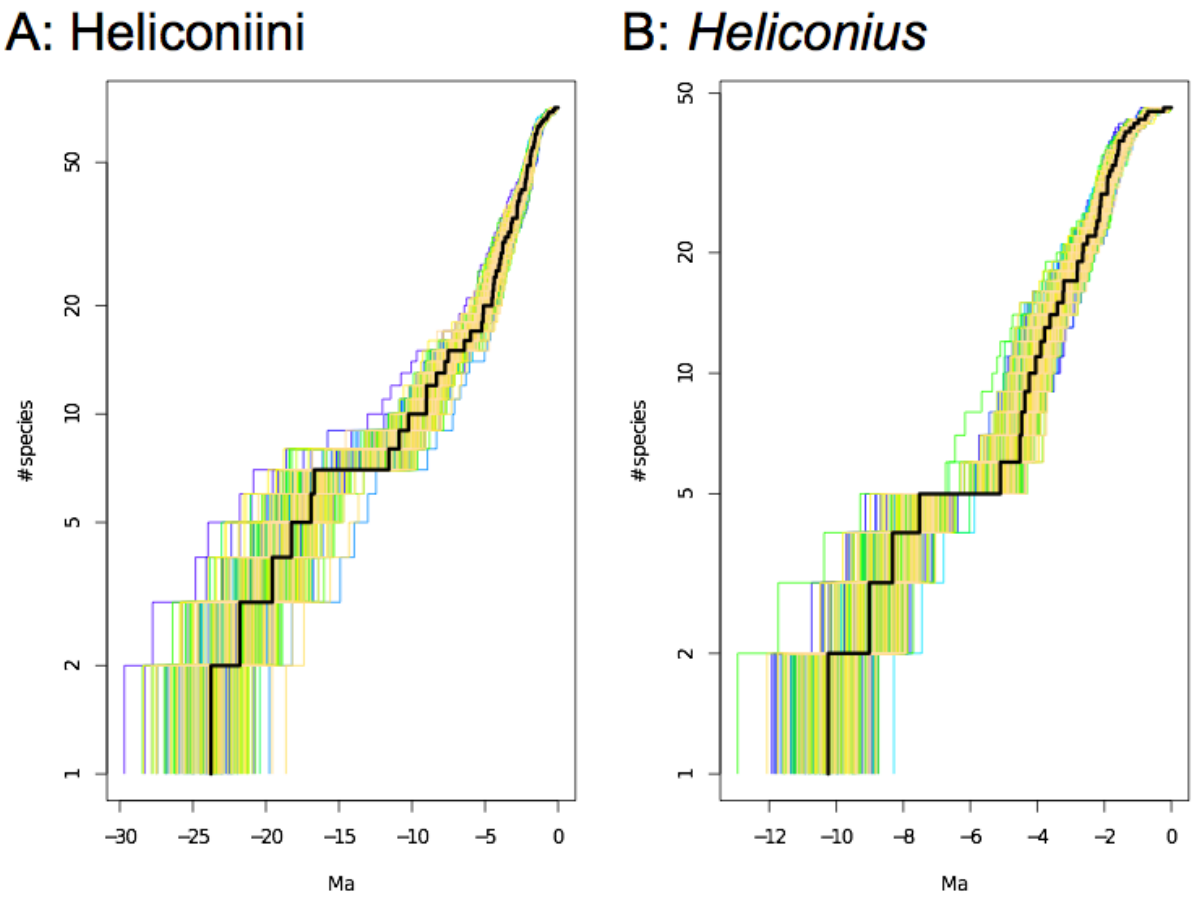

928

929 Figure 5. Lineage through time (LTT) plots based on the calibrated, uncorrelated molecular clock
930 analysis in BEAST. A. Semilogarithmic LTT plot of the Heliconiini butterflies with the maximum
931 clade credibility phylogeny in black and a random sample of 200 posterior trees around. B. LTT
932 plot for *Heliconius*.

933

934

935

936

937

938

939

940

941 TABLES

Marker	Name	Type	Chromosome	Length (bp)[a]	#Variable sites[a]	# Pars. Inf.[a]	Model: full dataset	Model: single-individual	Model: *BEAST
CoI/II, codon 1+2	*cytochrome oxidase I/II*	mt CDS	mitochondrion	1589	265	190	GTR+G	GTR+G	GTR+I
CoI/II, codon 3	*cytochrome oxidase I/II*	mt CDS	mitochondrion	745	666	611	GTR+G	GTR+G	GTR+G
tRNA-Leu	*Leucine tRNA*	tRNA	mitochondrion	77	17	8	Concatenated with *CoI/II*, codon 1+2		
16S	*ribosomal subunit 16*	rDNA	mitochondrion	533	160	128	GTR+G	GTR+G	GTR+G
Aact	*acetoacetyl CoA-thiolase*	nuclear exon	18	743	235	160	GTR+G	GTR+G	GTR+G
ArgK	*arginine kinase*	nuclear exon	10	608	199	162	SYM+G	GTR+G	GTR+G
Cad	*carbamyl P-synthetase*	nuclear exon	20	810	311	256	GTR+G	GTR+G	GTR+G
Cat	*catalase*	nuclear exon	Z	739	270	211	HKY+G	GTR+G	GTR+G
Cmdh	*cytosolic malate dehydrogenase*	nuclear exon	19	790	292	232	GTR+G	HKY+G	GTR+G
Ddc	*dopadecarboxylase*	nuclear exon	1	339	140	108	GTR+G	GTR+G	HKY+G
Dpp	*decapentaplegic*	nuclear exon	19	315	111	93	HKY+G	GTR+G	HKY+G
Ef1a	*elongation factor 1a*	nuclear exon	10	1189	330	262	GTR+G	HKY+G	GTR+I
Gapdh	*glyceraldehyde 3-phosphate dehydrogenase*	nuclear exon	5	722	229	181	GTR+G	GTR+G	GTR+G
Gts	*glycyl-tRNA synthetase*	nuclear exon	11	936	333	218	GTR+G	GTR+G	GTR+G
Hcl	*hairy cell leukemia protein*	nuclear exon	18	761	203	137	GTR+G	HKY+G	GTR+G
Hsp40	*heat shock protein 40*	nuclear exon	10	539	194	149	GTR+G	GTR+G	HKY+G
Idh	*isocitrate dehydrogenase*	nuclear exon	20	678	251	223	GTR+G	GTR+G	HKY+G
Lam	*laminin*	nuclear exon	17	880	306	191	GTR+G	GTR+G	GTR+G
Rps2	*ribosomal protein 2*	nuclear exon	17	419	142	115	GTR+G	GTR+G	GTR+G

Rps5	*ribosomal protein 5*	nuclear exon	11	615	192	154	GTR+G	GTR+G	GTR+G
Tada3	*transcriptional adaptor 3*	nuclear exon	5	757	285	234	GTR+G	GTR+G	GTR+G
Trh	*trachealess*	nuclear exon	9	677	258	227	GTR+G	SYM+G	GTR+G
Vas	*ATP synthase 21 kDa proteolipid subunit*	nuclear exon	13	723	192	136	GTR+G	GTR+G	HKY+I
Wg	*wingless*	nuclear exon	1	374	181	137	SYM+G	GTR+G	GTR+G

943

944 Table 1. Position in the genome, variability statistics and models of sequence evolution for two mitochondrial and 20 nuclear markers used in the

945 study. Statistics are reported for the core alignment including outgroups.

946

947

Grouping	Likelihood	ELW probability	SH result
ML tree	-142583	0.117	
Cethosia+Heliconiini	-142594	0.048	
Agraulis+*Dione* basal	-142599	0.006	
basal genera monophyletic	-142596	0.025	
Dryas+*Dryadula* monophyletic	-142593	0.058	
Neruda not in *Heliconius*	-142636	0.000	$p<0.05$
Laparus not in *Heliconius*	-143233	0.000	$p<0.05$
H. erato monophyletic	-142592	0.114	
H. ricini basal to *H. demeter*	-142590	0.084	
H. antiochus basal to *H sara*	-142588	0.170	
primitive clade monophyletic	-142613	0.000	$p<0.05$
H. wallacei monophyletic	-142584	0.115	
H. elevatus monophyletic	-142590	0.041	
H. cydno monophyletic	-142619	0.001	$p<0.05$
H. heurippa with *H. timareta*	-142586	0.209	
H. melpomene East+Guiana clade	-142620	0.011	$p<0.05$

Table 2. Maximum likelihood tests of alternative topologies. Phylogenies were estimated under constraints enforcing alternative topologies and compared to the original ML tree with the Shimodaira-Hasegawa test and the Expected Likelihood Weights test with 100 bootstrap replicates.

	Heliconius vs *Eueides*	*Heliconius* vs *Agraulis*	*Heliconius* vs *Philaethria*	*H. melpomene* vs *H. erato*	*H. erato* vs *H. hecalesia*
Mallet et al. 2007	11.0	13.0	14.5	9.5	4.0
Pohl et al. 2009	n/a	32.0 (40.0-24.0)	n/a	17.0 (11.0-23.0)	n/a
Wahlberg et al. 2009	18.5 (12.5-24.5)	26.5 (21-32)	30.0 (36.5-23.5)	n/a	n/a
Cuthill and Charleston 2012	13.0 (10.5-16.5)	n/a	n/a	10.5 (8-13.5)	4.5 (2.8-6.3)
BEAST	16.7 (14.1-19.5)	21.8 (18.6-25.5)	23.8 (20.3-27.7)	10.2 (8.7-12.0)	3.6 (3.0-4.4)
*BEAST	17.5 (11.6-23.4)	n/a	n/a	10.6 (14.9-6.7)	n/a

Table 3. Mean split ages in Ma at different levels of divergence within Heliconiini, as estimated by previous studies and by two Bayesian relaxed clock methods in the present work. Mean ages and 95% confidence intervals are reported where available.

982

Model	λ	λ_2	μ	μ_2	K	K_2	-lnL	AICc	wAIC
Heliconiini									
PB	0.23						-158.48	319.01	0.00
PB, shift 3.5 Ma	0.17	0.31					-155.43	315.04	0.00
PB, shift 4.5 Ma	0.13	0.33					-152.27	308.72	0.03
PB, shift 11 Ma	0.11	0.26					-155.57	315.32	0.00
PB, shift 12 Ma	0.11	0.25					-155.82	315.81	0.00
PB, any shift	0.12	0.32					-151.25	308.86	0.03
BD	0.38		0.26				-154.62	313.41	0.00
BD, shift 3.5 Ma	0.31	0.31	0.23	0.00			-153.50	315.61	0.00
BD, shift 4.5 Ma	0.16	0.33	0.04	0.00			-152.27	313.14	0.00
BD, shift 11 Ma	**0.19**	**0.40**	**0.02**	**0.26**			**-146.70**	**302.00**	**0.92**
BD, shift 12 Ma	0.21	0.37	0.02	0.25			-151.85	312.32	0.01
BD, any shift	0.26	0.37	0.16	0.23			-153.82	318.56	0.00
DD-E	0.23				Inf		-158.48	321.13	0.00
DDE1	0.35		0.20		$16x10^5$		-154.27	314.90	0.00
DDE5	0.36		0.24		2190		-153.64	313.63	0.00
DDE1, shift 3.5 Ma	0.31	0.42	0.23	0.00	7912	208	-153.41	320.13	0.00
DDE1, shift 4.5 Ma	0.15	0.45	0.04	0.01	Inf	171	-151.97	317.25	0.00
DDE1, shift 11 Ma	0.94	0.75	0.40	0.38	33	68	-155.09	323.49	0.00
DDE1, shift 12 Ma	0.17	0.30	0.00	0.07	26	941	-154.36	322.02	0.00
DDE1, any shift	0.16	0.49	0.01	0.07	71	152	-151.18	318.13	0.00
Heliconius									
PB	**0.42**						**-73.87**	**149.82**	**0.30**

PB, shift 3.5 Ma	0.38	0.44					-73.77	151.82	0.11
PB, shift 4.5 Ma	**0.26**	**0.47**					**-72.79**	**149.86**	**0.30**
BD	0.43		0.02				-73.86	152.00	0.10
BD, shift 3.5 Ma	0.60	0.44	0.39	0.00			-73.26	155.50	0.02
BD, shift 4.5 Ma	0.26	0.47	0.00	0.00			-72.79	154.56	0.03
DD-E	0.42				Inf		-73.87	152.01	0.10
DDE1	0.45		0.07		$6x10^5$		-73.88	154.34	0.03
DDE5	0.43		0.02		Inf		-73.86	156.70	0.01
DDE1, shift 3.5 Ma	0.39	0.60	0.02	0.00	$11x10^6$	111	-73.51	161.16	0.00
DDE1, shift 4.5 Ma	0.26	0.70	0.00	0.00	Inf	85	-72.18	158.51	0.00
DDE1, any shift	0.38	0.45	0.01	0.00	128	9710	-73.79	164.53	0.00

Table 4. Results of diversification model fitting to the maximum clade credibility chronograms of Heliconiini and *Heliconius*, estimated under a relaxed molecular clock model in BEAST. Models are compared in terms of corrected AIC (AICc) and relative Akaike weights (wAIC). Models: PB=Pure Birth, BD=Birth-Death, DD-E=Diversity Dependence without Extinction, DD+E1=Diversity Dependence with Extinction and a linear scaling of speciation term, DD+E5=Linear Dependence With Extinction and linear scaling terms for speciation and extinction. Where indicated, models include shifts in speciation and extinction rates at fixed times, or at any time.

998 REFERENCES

999 Akaike H. 1974. A new look at the statistical model identification. IEEE Trans. Automat. Contr.
1000 19:716–723.

1001 Alfaro M.E., Santini F., Brock C., Alamillo H., Dornburg A., Rabosky D.L., Carnevale G., Harmon
1002 L.J. 2009. Nine exceptional radiations plus high turnover explain species diversity in jawed
1003 vertebrates. Proc. Natl. Acad. Sci. U. S. A. 106:13410–4.

1004 Anderson C.N.K., Liu L., Pearl D., Edwards S. V 2012. Tangled trees: the challenge of inferring
1005 species trees from coalescent and noncoalescent genes. Methods Mol. Biol. 856:3–28.

1006 Ané C., Larget B., Baum D. a, Smith S.D., Rokas A. 2007. Bayesian estimation of concordance
1007 among gene trees. Mol. Biol. Evol. 24:412–26.

1008 Antonelli A., Nylander J.A.A., Persson C., Sanmartı I. 2009. Tracing the impact of the Andean
1009 uplift on Neotropical plant evolution. Proc. Natl. Acad. Sci. U. S. A. 106:9749-9754.

1010 Arias C.F., Muñoz A.G., Jiggins C.D., Mavárez J., Bermingham E., Linares M. 2008. A hybrid
1011 zone provides evidence for incipient ecological speciation in Heliconius butterflies. Mol.
1012 Ecol. 17:4699–712.

1013 Barão K.R., Gonçalves G.L., Mielke O.H.H., Kronforst M.R., Moreira G.R.P. 2014. Species
1014 boundaries in *Philaethria* butterflies: an integrative taxonomic analysis based on genitalia
1015 ultrastructure, wing geometric morphometrics, DNA sequences, and amplified fragment
1016 length polymorphisms. Zool. J. Linn. Soc. 170:690-709.

1017 Barker F.K., Burns K.J., Klicka J., Lanyon S.M., Lovette I.J. 2013. Going to extremes: contrasting
1018 rates of diversification in a recent radiation of new world passerine birds. Syst. Biol. 62:298–
1019 320.

1020 Bates H. W. 1862. Contributions to an insect fauna of the Amazon valley. Lepidoptera:
1021 Heliconidae. Trans. Linn. Soc. London 23:495-566.

1022 Bates H.W. 1863. The Naturalist on the River Amazons. London: John Murray.

1023 Baum D.A. 2007. Concordance trees, concordance factors, and the exploration of reticulate

1024 genealogy. Taxon. 56:417–426.
1025 Baxter S.W., Johnston S.E., Jiggins C.D. 2009. Butterfly speciation and the distribution of gene
1026 effect sizes fixed during adaptation. Heredity. 102:57–65.
1027 Belfiore N.M., Liu L., Moritz C. 2008. Multilocus phylogenetics of a rapid radiation in the genus
1028 Thomomys (Rodentia: Geomyidae). Syst. Biol. 57:294–310.
1029 Beltrán M., Jiggins C.D., Brower A.V.Z., Bermingham E., Mallet J. 2007. Do pollen feeding,
1030 pupal-mating and larval gregariousness have a single origin in Heliconius butterflies? Sorting
1031 Inferences from multilocus DNA sequence data. Bio. J. Linn. Soc. 92:221–239.
1032 Beltrán M., Jiggins C.D., Bull V., Linares M., Mallet J., McMillan W.O., Bermingham E. 2002.
1033 Phylogenetic discordance at the species boundary: comparative gene genealogies among
1034 rapidly radiating Heliconius butterflies. Mol. Biol. Evol. 19:2176–90.
1035 Benitez-Vieyra S., Hempel de Ibarra N., Wertlen A.M., Cocucci A.A. 2007. How to look like a
1036 mallow: evidence of floral mimicry between Turneraceae and Malvaceae. Proc. Biol. Sci.
1037 274:2239–48.
1038 Benson W.W. 1972. Natural selection for Müllerian mimicry in heliconius erato in Costa Rica.
1039 Science. 176:936–939.
1040 Benson, W. W. ., Brown, K. S., & Gilbert, L. E. . G. (1975). Coevolution of Plants and
1041 Herbivores: Passion Flower Butterflies. *Evolution*, *29*(4), 659–680.
1042 Biomatters Ltd 2012. Geneious. http://www.geneious.com
1043 Bouckaert R.R. 2010. DensiTree: making sense of sets of phylogenetic trees. Bioinformatics.
1044 26:1372–3.
1045 Brandley M.C., Wang Y., Guo X., Oca A.N.M., Fería-Ortíz M., Hikida T., Ota H. 2011.
1046 Accommodating heterogenous rates of evolution in molecular divergence dating methods: an
1047 example using intercontinental dispersal of Plestiodon (Eumeces) lizards. Syst. Biol. 60:3–15.
1048 Briscoe A.D., Muños A.M., Kozak K.M., Walters J.R., Yuan F., Jamie G.A., Martin S.H.,
1049 Dasmahapatra K., Ferguson L.C., Mallet J., Jacquin-Joly, Emmanuelle Jiggins C.D. 2013.

1050 Female Behaviour Drives Expression and Evolution of Gustatory Receptors in Butterflies.
1051 PLoS Genet. 9(7).
1052 Brodie III E.D., Brodie Jr E.D. 2004. Venomous snake mimicry. In: Campbell J.A., Lamar W.W.
1053 The venomous reptiles of the western hemisphere, Vol. II. Ithaca, NY: Comstock Publishing
1054 Associates. p. 617–633.
1055 Brower a V 1994a. Rapid morphological radiation and convergence among races of the butterfly
1056 Heliconius erato inferred from patterns of mitochondrial DNA evolution. Proc. Natl.
1057 Acad. Sci. U. S. A. 91:6491–5.
1058 Brower a. V.Z. 1994b. Phylogeny of Heliconius butterflies inferred from mitochondrial DNA
1059 sequences (Lepidoptera: Nymphalidae). Mol. Phylogenet. Evol. 3:159 –174.
1060 Brower a. V.Z., Egan M.G. 1997. Cladistic analysis of Heliconius butterflies and relatives
1061 (Nymphalidae: Heliconiiti): a revised phylogenetic position for Eueides based on sequences
1062 from mtDNA and a nuclear gene. Proc. R. Soc. B Biol. Sci. 264:969–977.
1063 Brower A.V.Z. 1997. The evolution of ecologically important characters in Heliconius butterflies
1064 (Lepidoptera: Nymphalidae): a cladistic review. Zoo. J. Linn. Soc. 119: 457-472.
1065 Brown K., Sheppard P., Turner J. 1974. Quaternary refugia in tropical america: Evidence from race
1066 formation in Heliconius butterflies. Proc. R. Soc. London. Ser. B, Biol. Sci. 187:369–378.
1067 Brown K.S. 1981. The Biology of Heliconius and Related Genera. Annu. Rev. Entomol. 26:427–
1068 457.
1069 Brumfield R.T., Edwards S. V 2007. Evolution into and out of the Andes: a Bayesian analysis of
1070 historical diversification in Thamnophilus antshrikes. Evolution. 61:346–67.
1071 Burbrink, F. T., & Pyron, R. A. (2011). The impact of gene-tree/species-tree discordance on
1072 diversification-rate estimation. *Evolution; international journal of organic evolution*, *65*(7),
1073 1851–61. doi:10.1111/j.1558-5646.2011.01260.x
1074 Bybee S.M., Yuan F., Ramstetter M.D., Llorente-Bousquets J., Reed R.D., Osorio D., Briscoe A.D.
1075 2012. UV photoreceptors and UV-yellow wing pigments in Heliconius butterflies allow a

color signal to serve both mimicry and intraspecific communication. Am. Nat. 179:38–51.

Camacho C., Coulouris G., Avagyan V., Ma N., Papadopoulos J., Bealer K., Madden T.L. 2009. BLAST+: architecture and applications. BMC Bioinformatics. 10:421.

Cardoso M.Z., Gilbert L.E. 2013. Pollen feeding, resource allocation and the evolution of chemical defence in passion vine butterflies. J. Evol. Biol. 26:1254–60.

Ceccarelli F.S., Crozier R.H. 2007. Dynamics of the evolution of Batesian mimicry: molecular phylogenetic analysis of ant-mimicking Myrmarachne (Araneae: Salticidae) species and their ant models. J. Evol. Biol. 20:286–95.

Chauhan R., Jones R., Wilkinson P., Pauchet Y., Ffrench-Constant R.H. 2013. Cytochrome P450-encoding genes from the Heliconius genome as candidates for cyanogenesis. Insect Mol. Biol. 22:532–40.

CLCBio 2012. CLC Genomics Workbench. http://www.clcbio.com/products/clc-genomics-workbench/

CodonCode Corporation 2012. CodonCode. http://www.codoncode.com/

Colinvaux, P. A., De Oliveira, P. E., & Bush, M. B. (2000). Amazonian and neotropical plant communities on glacial time-scales: The failure of the aridity and refuge hypotheses. *Quaternary Science Reviews*, *19*(1-5), 141–169.

Constantino L.M., Salazar J.A. 2010. A review of the Philaethria dido species complex (Lepidoptera: Nymphalidae: Heliconiinae) and description of three new sibling species from Colombia. Zootaxa. 27:1– 27.

Colinvaux P.A., De Oliveira P.E., Bush M.B. 2000. Amazonian and neotropical plant communities on glacial timescales: The failure of the aridity and refuge hypotheses. Quat. Sci. Rev. 19:141–169.

Cuthill J.H., Charleston M. 2012. Phylogenetic codivergence supports coevolution of mimetic Heliconius butterflies. PLoS One. 7:e36464.

1102 Cutter A.D. 2013. Integrating phylogenetics, phylogeography and population genetics through
1103 genomes and evolutionary theory. Mol. Phylogenet. Evol. 69:1172–1185.
1104 Dasmahapatra K.K., Lamas G., Simpson F., Mallet J. 2010. The anatomy of a “suture zone” in
1105 Amazonian butterflies: a coalescent-based test for vicariant geographic divergence and
1106 speciation. Mol. Ecol. 19:4283-4301.
1107 Day J.J., Peart C.R., Brown K.J., Friel J.P., Bills R., Moritz T. 2013. Continental diversification of
1108 an African catfish radiation (Mochokidae: Synodontis). Syst. Biol. 62:351–65.
1109 Degnan J.H., Rosenberg N. a 2006. Discordance of species trees with their most likely gene trees.
1110 PLoS Genet. 2:e68.
1111 Derryberry E.P., Claramunt S., Derryberry G., Chesser R.T., Cracraft J., Aleixo A., Pérez-Emán J.,
1112 Remsen J. V., Brumfield R.T. 2011. Lineage diversification and morphological evolution in a
1113 large-scale continental radiation: the neotropical ovenbirds and woodcreepers (aves:
1114 Furnariidae). Evolution. 65:2973–86.
1115 Drummond A.J., Rambaut A. 2007. BEAST: Bayesian evolutionary analysis by sampling trees.
1116 BMC Evol. Biol. 7:214.
1117 Drummond A.J., Rambaut A., Xie W. 2010. BEAuti. http://www.**beast**.bio.ed.ac.uk
1118 Duenez-Guzman E. a, Mavárez J., Vose M.D., Gavrilets S. 2009. Case studies and mathematical
1119 models of ecological speciation. 4. Hybrid speciation in butterflies in a jungle. Evolution.
1120 63:2611–26.
1121 Edgar R.C. 2004. MUSCLE: multiple sequence alignment with high accuracy and high throughput.
1122 Nucleic Acids Res. 32:1792–7.
1123 Edwards S. V 2009. Is a new and general theory of molecular systematics emerging? Evolution.
1124 63:1–19.
1125 Edwards S. V, Liu L., Pearl D.K. 2007. High-resolution species trees without concatenation. Proc.
1126 Natl. Acad. Sci. U.S.A. 104:5936–41.
1127 Elde N.C., Malik H.S. 2009. The evolutionary conundrum of pathogen mimicry. Nat. Rev.

1128 Microbiol. 7:787–97.
1129 Elias M., Gompert Z., Jiggins C., Willmott K. 2008. Mutualistic interactions drive ecological niche
1130 convergence in a diverse butterfly community. PLoS Biology. 6:2642–9.
1131 Elias M., Gompert Z., Willmott K., Jiggins C. 2009. Phylogenetic community ecology needs to take
1132 positive interactions into account: Insights from colourful butterflies. Commun. Integr. Biol.
1133 2:113–6.
1134 Emsley M.G. 1965. Speciation in Heliconius (Lep., Nymphalidae): morphology and geographic
1135 distribution. Zoologica. 50:191–254.
1136 Estrada C., Schulz S., Yildizhan S., Gilbert L.E. 2011. Sexual selection drives the evolution of
1137 antiaphrodisiac pheromones in butterflies. Evolution (N. Y). Evolution. 65:2843-2854.
1138 Etienne R.S., Haegeman B. 2012. A conceptual and statistical framework for adaptive radiations
1139 with a key role for diversity dependence. Am. Nat. 180:E75–89.
1140 Etienne R.S., Haegeman B., Stadler T., Aze T., Pearson P.N., Purvis A., Phillimore A.B. 2012.
1141 Diversity -dependence brings molecular phylogenies closer to agreement with the fossil
1142 record. Proc. Biol. Sci. 279:1300–9.
1143 Figueiredo, J., Hoorn, C., Van der Ven, P., & Soares, E. (2009). Late Miocene onset of the Amazon
1144 River and the Amazon deep-sea fan: Evidence from the Foz do Amazonas Basin. *Geology*,
1145 *37*(7), 619–622.
1146 Flanagan N.S., Tobler a, Davison a, Pybus O.G., Kapan D.D., Planas S., Linares M., Heckel D.,
1147 McMillan W.O. 2004. Historical demography of Mullerian mimicry in the neotropical
1148 Heliconius butterflies. Proc. Natl. Acad. Sci. U. S. A. 101:9704–9.
1149 Fordyce J. A. 2010. Host shifts and evolutionary radiations of butterflies. Proc. Biol. Sci. 277:3735–
1150 43.
1151 Fulton T.L., Strobeck C. 2009. Multiple markers and multiple individuals refine true seal phylogeny
1152 and bring molecules and morphology back in line. Proc. R. Soc. B Biol. Sci. 277:1065–1070.
1153 Gatesy J., Baker R.H. 2005. Hidden likelihood support in genomic data: can forty-five wrongs

1154 make a right? Syst. Biol. 54:483–92.
1155 Gatesy J., DeSalle R., Wahlberg N. 2007. How many genes should a systematist sample?
1156 Conflicting insights from a phylogenomic matrix characterized by replicated incongruence.
1157 Syst. Biol. 56:355–63.
1158 Gatesy J., Springer M.S. 2013. Concatenation versus coalescence versus "concatalescence". Proc.
1159 Natl. Acad. Sci. U. S. A. 110:E1179.
1160 Gerard D., Gibbs H.L., Kubatko L. 2011. Estimating hybridization in the presence of coalescence
1161 using phylogenetic intraspecific sampling. BMC Evol. Biol. 11:291.
1162 Gregory-Wodzicki K.M. 2000. Uplift history of the Central and Northern Andes: A review. Geol.
1163 Soc. Am. Bull. 112:1091–1105.
1164 Hall, J. P. W., & Harvey, D. J. (2002). The phylogeogrpahy of Amazonia revisited: New evidence
1165 from Riodinid butterflies. *Evolution*, *56*(7), 1489–1497.
1166 Heled J., Drummond A.J. 2010. Bayesian inference of species trees from multilocus data. Mol.
1167 Biol. Evol. 27:570–80.
1168 Heliconius Genome Consortium 2012. Butterfly genome reveals promiscuous exchange of
1169 mimicry adaptations among species. Nature. 487:94–98.
1170 Hill, R. I., Gilbert, L. E., & Kronforst, M. R. (2013). Cryptic genetic and wing pattern diversity in a
1171 mimetic Heliconius butterfly. *Molecular ecology*, *22*(10), 2760–70.
1172 Hillis D.M., Heath T.A., St. John K. 2005. Analysis and Visualization of Tree Space. Syst. Biol.
1173 54:471 – 482.
1174 Hines H.M., Counterman B.A., Papa R., Albuquerque de Moura P., Cardoso M.Z., Linares M.,
1175 Mallet J., Reed R.D., Jiggins C.D., Kronforst M.R., McMillan W.O. 2011. Wing patterning
1176 gene redefines the mimetic history of Heliconius butterflies. Proc. Natl. Acad. Sci. U. S. A.
1177 108:19666–71.
1178 Hines H.M., Williams P.H. 2012. Mimetic colour pattern evolution in the highly polymorphic
1179 Bombus trifasciatus (Hymenoptera: Apidae) species complex and its comimics. Zool. J. Linn.

1180 Soc. 166:805–826.
1181 Holland B.R., Huber K.T., Dress A., Moulton V. 2002. Delta plots: a tool for analyzing
1182 phylogenetic distance data. Mol. Biol. Evol. 19:2051–9.
1183 Hoorn C., Wesselingh F.P., ter Steege H., Bermudez M.A., Mora A., Sevink J., Sanmartín I.,
1184 Sanchez-Meseguer A., Anderson C.L., Figueiredo J.P., Jaramillo C., Riff D., Negri F.R.,
1185 Hooghiemstra H., Lundberg J., Stadler T., Särkinen T., Antonelli A. 2010. Amazonia through
1186 time: Andean uplift, climate change, landscape evolution, and biodiversity. Science. 330:927–
1187 31.
1188 Janzen D.H., Hallwachs W., Burns J.M. 2010. A tropical horde of counterfeit predator eyes. Proc.
1189 Natl. Acad. Sci. U. S. A. 107:11659–65.
1190 Jaramillo, C., Hoorn, C., Silva, S. A. F., Leite, F., Herrera, F., Quiroz, L., Rodolfo, D., et al. (2010).
1191 The origin of the modern Amazon rainforest: implications of the palynological and
1192 palaeobotanical record. In C. Hoorn & F. P. Wesselingh (Eds.), *Amazonia, Landscape and*
1193 *Species Evolution: A Look into the Past* (1st ed., pp. 317–334). Oxford: Blackwell.
1194 Jiggins C.D., Naisbit R.E., Coe R.L., Mallet J. 2001. Reproductive isolation caused by colour
1195 pattern mimicry. Nature. 411:302–5.
1196 Jiggins C.D. 2008. Ecological Speciation in Mimetic Butterflies. BioScience. 58:541.
1197 Jiggins C.D., Salazar C., Linares M., Mavarez J. 2008. Review. Hybrid trait speciation and
1198 Heliconius butterflies. Philos. Trans. R. Soc. Lond. B. Biol. Sci. 363:3047–54.
1199 Jones R.T., Le Poul Y., Whibley A.C., Mérot C., ffrench-Constant R.H., Joron M. 2013. Wing
1200 shape variation associated with mimicry in butterflies. Evolution. 67:2323–34.
1201 Jones R.T., Salazar P.A., ffrench-Constant R.H., Jiggins C.D., Joron M. 2012. Evolution of a
1202 mimicry supergene from a multilocus architecture. Proc. Biol. Sci. 279:316–25.
1203 Katoh K. 2002. MAFFT: a novel method for rapid multiple sequence alignment based on fast
1204 Fourier transform. Nucleic Acids Res. 30:3059–3066.
1205 Kloepper T.H., Huson D.H. 2008. Drawing explicit phylogenetic networks and their integration into

1206 SplitsTree. BMC Evol. Biol. 8:22.
1207 Knowles L., Kubatko L. 2010. Estimating species trees. Estimating species trees: practical and
1208 theoretical aspects. Hoboken: John Wiley & Sons. p. 1–15.
1209 Kubatko L., Meng C. 2010. Accomodating hybridisation in a multilocus phylogenetic framework.
1210 Estimating species trees: practical and theoretical aspects. Hoboken: John Wiley & Sons. p.
1211 99–114.
1212 Kunte K., Shea C., Aardema M.L., Scriber J.M., Juenger T.E., Gilbert L.E., Kronforst M.R. 2011.
1213 Sex chromosome mosaicism and hybrid speciation among tiger swallowtail butterflies. PLoS
1214 Genet. 7:e1002274.
1215 Lamas G., Callaghan C., Casagrande M., Mielke O., Pyrcz T., Robbins R., Viloria. A. 2004.
1216 Hesperioidea -- Papilionoidea. In: Heppner J. Atlas of Neotropical Lepidoptera. Checklist:
1217 part 4A. Gainesville, Florida: Association for Tropical Lepidoptera/Scientific Publishers.
1218 Larget B.R., Kotha S.K., Dewey C.N., Ané C. 2010. BUCKy: gene tree/species tree reconciliation
1219 with Bayesian concordance analysis. Bioinformatics. 26:2910–1.
1220 Leaché A.D., Harris R.B., Rannala B., Yang Z. 2014. The Influence of Gene Flow on Species Tree
1221 Estimation: A Simulation Study. Syst. Biol. 63:17-30.
1222 Leaché A.D., Rannala B. 2010. The Accuracy of Species Tree Estimation under Simulation: A
1223 Comparison of Methods. Syst. Biol. 1–12.
1224 Lee C.S., McCool B.A., Moore J.L., Hillis D.M., Gilbert L.E. 1992. Phylogenetic study of
1225 heliconiine butterflies based on morphology and restriction analysis of ribosomal RNA genes.
1226 Zool. J. Linn. Soc. 106:17–31.
1227 Lee J.Y., Joseph L., Edwards S. V 2012. A species tree for the Australo-Papuan Fairy-wrens and
1228 allies (Aves: Maluridae). Syst. Biol. 61:253–71.
1229 Leigh J.W., Susko E., Baumgartner M., Roger A.J. 2008. Testing congruence in phylogenomic
1230 analysis. Syst. Biol. 57:104–15.
1231 Lewis, A. R., Marchant, D. R., Ashworth, A. C., Hemming, S. R., & Machlus, M. L. (2007). Major

middle Miocene global climate change: Evidence from East Antarctica and the Transantarctic Mountains. *Geological Society of America Bulletin*, *119*(11-12), 1449–1461.

Linnen C.R., Farrell B.D. 2008. Comparison of methods for species-tree inference in the sawfly genus Neodiprion (Hymenoptera: Diprionidae). Syst. Biol. 57:876–90.

Maddison W.P. 1997. Gene Trees in Species Trees. Syst. Biol. 46:523–536.

Maddison W.P., Knowles L.L. 2006. Inferring phylogeny despite incomplete lineage sorting. Syst. Biol. 55:21–30.

Maddison W.P., Maddison D.R. 2011. Mesquite: a modular system for evolutionary analysis. http://www.mesquiteproject.org

Mallet J., Barton N.H. 1989. Strong Natural Selection in a Warning-Color Hybrid Zone. Evolution. 43:421.

Mallet J., Beltrán M., Neukirchen W., Linares M. 2007. Natural hybridization in heliconiine butterflies: the species boundary as a continuum. BMC Evol. Biol. 7:28.

Mallet J., Joron M. 1999. Evolution of diversity in warning color and mimicry: polymorphisms, shifting balance, and speciation. Annual Review of Ecology and Systematics. 30:201–233.

Mallet J., McMillan W., Jiggins C. 1998. Mimicry and warning color at the boundary between races and species. In: Howard D., Berlocher S. Endless Forms: Species and Speciation. New York: Oxford Univ. Press. p. 390–403.

Martin A., Papa R., Nadeau N.J., Hill R.I., Counterman B.A., Halder G., Jiggins C.D., Kronforst M.R., Long A.D., McMillan W.O., Reed R.D. 2012. Diversification of complex butterfly wing patterns by repeated regulatory evolution of a Wnt ligand. Proc. Natl. Acad. Sci. U. S. A. 109:12632–7.

Martin S.H., Dasmahapatra K.K., Nadeau N.J., Salazar C., Walters J.R., Simpson F., Blaxter M., Manica A., Mallet J., Jiggins C.D. 2013. Genome-wide evidence for speciation with gene flow in Heliconius butterflies. Genome Res. 23:1817-1828.

Mavárez J., Salazar C. a, Bermingham E., Salcedo C., Jiggins C.D., Linares M. 2006. Speciation by

1258 hybridization in Heliconius butterflies. Nature. 441:868–71.
1259 McMillan W.O., Jiggins C.D., Mallet J. 1997. What initiates speciation in passion-vine butterflies?
1260 Proc. of the Natl. Acad. of Sci. U.S.A. 94:8628–33.
1261 Mérot C., Mavárez J., Evin A., Dasmahapatra K.K., Mallet J., Lamas G., Joron M. 2013. Genetic
1262 differentiation without mimicry shift in a pair of hybridizing Heliconius species (Lepidoptera:
1263 Nymphalidae). Biol. J. Linn. Soc. 109:830–847.
1264 Merrill R.M., Naisbit R.E., Mallet J., Jiggins C.D. 2013. Ecological and genetic factors influencing
1265 the transition between host-use strategies in sympatric Heliconius butterflies. J. Evol. Biol.
1266 26:1959–67.
1267 Merrill R.M., Wallbank R.W.R., Bull V., Salazar P.C.A., Mallet J., Stevens M., Jiggins C.D. 2012.
1268 Disruptive ecological selection on a mating cue. Proc. Biol. Sci. 279:4907–13.
1269 Moreira G.R.P., Mielke C.G.C. 2010. A new species of Neruda Turner, 1976 from northeast Brazil
1270 (Lepidoptera: Nymphalidae, Heiconiinae, Heliconiini). Nachrichten des Entomol. Vereins
1271 Apollo. 31:85–91.
1272 Müller C.J., Beheregaray L.B. 2010. Palaeo island-affinities revisited--biogeography and
1273 systematics of the Indo-Pacific genus Cethosia Fabricius (Lepidoptera: Nymphalidae). Mol.
1274 Phylogenet. Evol. 57:314–26.
1275 Nadeau N.J., Martin S.H., Kozak K.M., Salazar C., Dasmahapatra K.K., Davey J.W., Baxter S.W.,
1276 Blaxter M.L., Mallet J., Jiggins C.D. 2013. Genome-wide patterns of divergence and gene
1277 flow across a butterfly radiation. Mol. Ecol. 22:814–26.
1278 Nylander J.A.A. 2004. MrModelTest. http://www.abc.se/~nylander/
1279 Papadopoulou A., Anastasiou I., Vogler A.P. 2010. Revisiting the insect mitochondrial molecular
1280 clock: the mid-Aegean trench calibration. Mol. Biol. Evol. 27:1659–72.
1281 Paradis E., Claude J., Strimmer K. 2004. APE: Analyses of Phylogenetics and Evolution in R
1282 language. Bioinformatics. 20:289–90.
1283 Pardo-Díaz C., Salazar C., Baxter S.W., Mérot C., Figueiredo-Ready W., Joron M., McMillan

1284 W.O., Jiggins C.D. 2012. Adaptive Introgression across Species Boundaries in Heliconius
1285 Butterflies. PLoS Genet. 8:e1002752.
1286 Penney H.D., Hassall C., Skevington J.H., Abbott K.R., Sherratt T.N. 2012. A comparative analysis
1287 of the evolution of imperfect mimicry. Nature. 483:461–4.
1288 Penz C. 1999. Higher level phylogeny for the passion-vine butterflies (Nymphalidae, Heliconiinae)
1289 based on early stage and adult morphology. Zool. J. Linn. Soc. 127:277–344.
1290 Penz C.M., Peggie D. 2003. Phylogenetic relationships among Heliconiinae genera based on
1291 morphology (Lepidoptera: Nymphalidae). Syst. Entomol. 28:451–479.
1292 Pfennig D. 2012. Mimicry: Ecology, evolution, and development. Curr. Zool. 58:604–606.
1293 Pigot A.L., Phillimore A.B., Owens I.P.F., Orme C.D.L. 2010. The shape and temporal dynamics of
1294 phylogenetic trees arising from geographic speciation. Syst. Biol. 59:660–73.
1295 Pohl N., Sison-Mangus M.P., Yee E.N., Liswi S.W., Briscoe A.D. 2009. Impact of duplicate gene
1296 copies on phylogenetic analysis and divergence time estimates in butterflies. BMC Evol. Biol.
1297 9:99.
1298 Posada D., Crandall K.A. 1998. Bioinformatics Applications Note. MODELTEST□: testing the
1299 model of DNA substitution. Evolution. 14:817–818.
1300 Przeczek K., Mueller C., Vamosi S.M. 2008. The evolution of aposematism is accompanied by
1301 increased diversification. Integrative Zoology. 3:149–56.
1302 Pybus O.G., Harvey P.H. 2000. Testing macro-evolutionary models using incomplete molecular
1303 phylogenies. Proc. Biol. Sci. 267:2267–72.
1304 Quek S.-P., Counterman B. a, Albuquerque de Moura P., Cardoso M.Z., Marshall C.R., McMillan
1305 W.O., Kronforst M.R. 2010. Dissecting comimetic radiations in Heliconius reveals
1306 divergent histories of convergent butterflies. Proc. Natl. Acad. Sci. U. S. A. 107:7365–70.
1307 R Development Core Team 2008. R: A language and environment for statistical computing.
1308 http://www.r- project.org
1309 Rabosky D.L. 2006. LASER: a maximum likelihood toolkit for detecting temporal shifts in

1310 diversification rates from molecular phylogenies. Evol. Bioinform. Online. 2:273–6.
1311 Rabosky D.L., Lovette I.J. 2008. Explosive evolutionary radiations: decreasing speciation or
1312 increasing extinction through time? Evolution. 62:1866–75.
1313 Rambaut A. 2009. FigTree. Tree figure drawing tool. http://www.tree.bio.ed.ac.uk/software/figtree/
1314 Rambaut A., Drummond A.J. 2010. LogCombiner. http://www.beast.bio.ed.ac.uk
1315 Reid N.M., Hird S.M., Brown J.M., Pelletier T.A., McVay J.D., Satler J.D., Carstens B.C. 2013.
1316 Poor fit to the multispecies coalescent is widely detectable in empirical data. Syst. Biol.
1317 syt057.
1318 Robinson D.F., Foulds L.R. 1981. Comparison of phylogenetic trees. Math. Biosci. 53:131–147.
1319 Ronquist F., Huelsenbeck J.P. 2003. MrBayes 3: Bayesian phylogenetic inference under mixed
1320 models. Bioinformatics. 19:1572–1574.
1321 Rosser N., Phillimore A.B., Huertas B., Willmott K.R., Mallet J. 2012. Testing historical
1322 explanations for gradients in species richness in heliconiine butterflies of tropical America.
1323 Biol. J. Linn. Soc. 105:479–497.
1324 Roure B., Baurain D., Philippe H. 2013. Impact of missing data on phylogenies inferred from
1325 empirical phylogenomic data sets. Mol. Biol. Evol. 30:197–214.
1326 Rull V. 2011. Neotropical biodiversity: timing and potential drivers. Trends in Ecology &
1327 Evolution. 26:508–513.
1328 Salazar C., Baxter S.W., Pardo-Díaz C., Wu G., Surridge A., Linares M., Bermingham E., Jiggins
1329 C.D. 2010. Genetic evidence for hybrid trait speciation in Heliconius butterflies. PLoS Genet.
1330 6:e1000930.
1331 Salzberg S.L., Phillippy A.M., Zimin A., Puiu D., Magoc T., Koren S., Treangen T.J., Schatz M.C.,
1332 Delcher A.L., Roberts M., Marçais G., Pop M., Yorke J. a 2012. GAGE: A critical
1333 evaluation of genome assemblies and assembly algorithms. Genome Res. 22:557–67.
1334 Savage W.K., Mullen S.P. 2009. A single origin of Batesian mimicry among hybridizing
1335 populations of admiral butterflies (Limenitis arthemis) rejects an evolutionary reversion to the

1336 ancestral phenotype. Proc. Biol. Sci. 276:2557–65.
1337 Schluter D. 2000. The Ecology of Adaptive Radiation. Oxford: Oxford University Press
1338 Sheppard P.M., Turner J.R.G., Brown K.S., Benson W.W., Singer M.C. 1985. Genetics and the
1339 evolution of Müllerian mimicry in Heliconius butterflies. Philos. Trans. R. Soc. B Biol. Sci.
1340 308:433–610.
1341 Sherratt T.N. 2008. The evolution of Müllerian mimicry. Naturwissenschaften. 95:681–95.
1342 Shimodaira H., Hasegawa M. 1989. Letter to the Editor: Multiple comparisons of log-likelihoods
1343 with applications to phylogenetic inference. DNA Seq. 1114–1116.
1344 Simpson J.T., Wong K., Jackman S.D., Schein J.E., Jones S.J.M., Birol I. 2009. ABySS: a parallel
1345 assembler for short read sequence data. Genome Res. 19:1117–23.
1346 Smith B.T., Harvey M.G., Faircloth B.C., Glenn T.C., Brumfield R.T. 2013. Target capture and
1347 massively parallel sequencing of Ultraconserved Elements for comparative studies at shallow
1348 evolutionary timescales. Syst. Biol. syt061.
1349 Solomon S.E., Bacci M., Martins J., Vinha G.G., Mueller U.G. 2008. Paleodistributions and
1350 comparative molecular phylogeography of leafcutter ants (Atta spp.) provide new insight into
1351 the origins of Amazonian diversity. PLoS One. 3:e2738.
1352 Song S., Liu L., Edwards S. V, Wu S. 2012. Resolving conflict in eutherian mammal phylogeny
1353 using phylogenomics and the multispecies coalescent model. Proc. Natl. Acad. Sci. U. S. A.
1354 109:14942–7.
1355 Stadler T. 2011. Mammalian phylogeny reveals recent diversification rate shifts. Proc. Natl. Acad.
1356 Sci. U. S. A. 108:6187–92.
1357 Stadler T. 2013. Recovering speciation and extinction dynamics based on phylogenies. J. Evol.
1358 Biol. 26:1203–19.
1359 Stamatakis A. 2006. RAxML-VI-HPC: maximum likelihood-based phylogenetic analyses with
1360 thousands of taxa and mixed models. Bioinformatics. 22:2688–90.
1361 Strimmer K., Rambaut A. 2002. Inferring confidence sets of possibly misspecified gene trees. Proc.

1362 Biol. Sci. 269:137–42.
1363 Supple M.A., Hines H.M., Dasmahapatra K.K., Lewis J.J., Nielsen D.M., Lavoie C., Ray D.A.,
1364 Salazar C., McMillan W.O., Counterman B.A. 2013. Genomic architecture of adaptive color
1365 pattern divergence and convergence in Heliconius butterflies. Genome Res. 23:1248–57.
1366 Swofford R. 2002. PAUP*: Phylogenetic Analysis Using Parsimony (*and other methods).
1367 http://www.**paup**.csit.fsu.edu
1368 Tamura K., Peterson D., Peterson N., Stecher G., Nei M., Kumar S. 2011. MEGA5: Molecular
1369 Evolutionary Genetics Analysis using Maximum Likelihood, Evolutionary Distance, and
1370 Maximum Parsimony Methods. Mol. Biol. Evol. 28:2731–2739.
1371 Than C., Ruths D., Nakhleh L. 2008. PhyloNet: a software package for analyzing and
1372 reconstructing reticulate evolutionary relationships. BMC Bioinformatics. 9:322.
1373 Turchetto-Zolet A.C., Pinheiro F., Salgueiro F., Palma-Silva C. 2013. Phylogeographical patterns
1374 shed light on evolutionary process in South America. Mol. Ecol. 22:1193–213.
1375 Turner J. 1965. Evolution of complex polymorphism and mimicry in distasteful South American
1376 butterflies. Proc. XII Int. Cong. Entomol. London. 267.
1377 Turner J.R., Johnson M.S., Eanes W.F. 1979. Contrasted modes of evolution in the same genome:
1378 allozymes and adaptive change in Heliconius. Proc. Natl. Acad. Sci. U. S. A. 76:1924–8.
1379 Vamosi S.M. 2005. On the role of enemies in divergence and diversification of prey: a review and
1380 synthesis. Can. J. Zoo. 83:894–910.
1381 Van Velzen R., Wahlberg N., Sosef M.S.M., Bakker F.T. 2013. Effects of changing climate on
1382 species diversification in tropical forest butterflies of the genus Cymothoe (Lepidoptera:
1383 Nymphalidae). Biol. J. Linn. Soc. 108:546–564.
1384 Wahlberg N., Leneveu J., Kodandaramaiah U., Peña C., Nylin S., Freitas A.V.L., Brower A.V.Z.
1385 2009. Nymphalid butterflies diversify following near demise at the Cretaceous/Tertiary
1386 boundary. Proc. Biol. Sci. 276:4295–302.
1387 Wahlberg N., Wheat C.W. 2008. Genomic outposts serve the phylogenomic pioneers: designing

novel nuclear markers for genomic DNA extractions of lepidoptera. Syst. Biol. 57:231–42.

Wertheim, J. O., & Sanderson, M. J. (2011). Estimating diversification rates: how useful are divergence times? Evolution. *65*(2), 309–20. doi:10.1111/j.1558-5646.2010.01159.x

Wiens J.J., Morrill M.C. 2011. Missing data in phylogenetic analysis: reconciling results from simulations and empirical data. Syst. Biol. 60:719–31.

Wilson J.S., Williams K.A., Forister M.L., von Dohlen C.D., Pitts J.P. 2012. Repeated evolution in overlapping mimicry rings among North American velvet ants. Nat. Commun. 3:1272.

Wright J.J. 2011. Conservative coevolution of Müllerian mimicry in a group of rift lake catfish. Evolution. 65:395–407.

Xia X., Xie Z. 2001. DAMBE: software package for data analysis in molecular biology and evolution. J. Hered. 92:371–3.

Yu Y., Than C., Degnan J.H., Nakhleh L. 2011. Coalescent histories on phylogenetic networks and detection of hybridization despite incomplete lineage sorting. Syst. Biol. 60:138–49.

Zhang W., Kunte K., Kronforst M.R. 2013. Genome-wide characterization of adaptation and speciation in tiger swallowtail butterflies using de novo transcriptome assemblies. Genome Biol. Evol. 5:1233–45.

1414 SUPPLEMENTARY FIGURES

1415

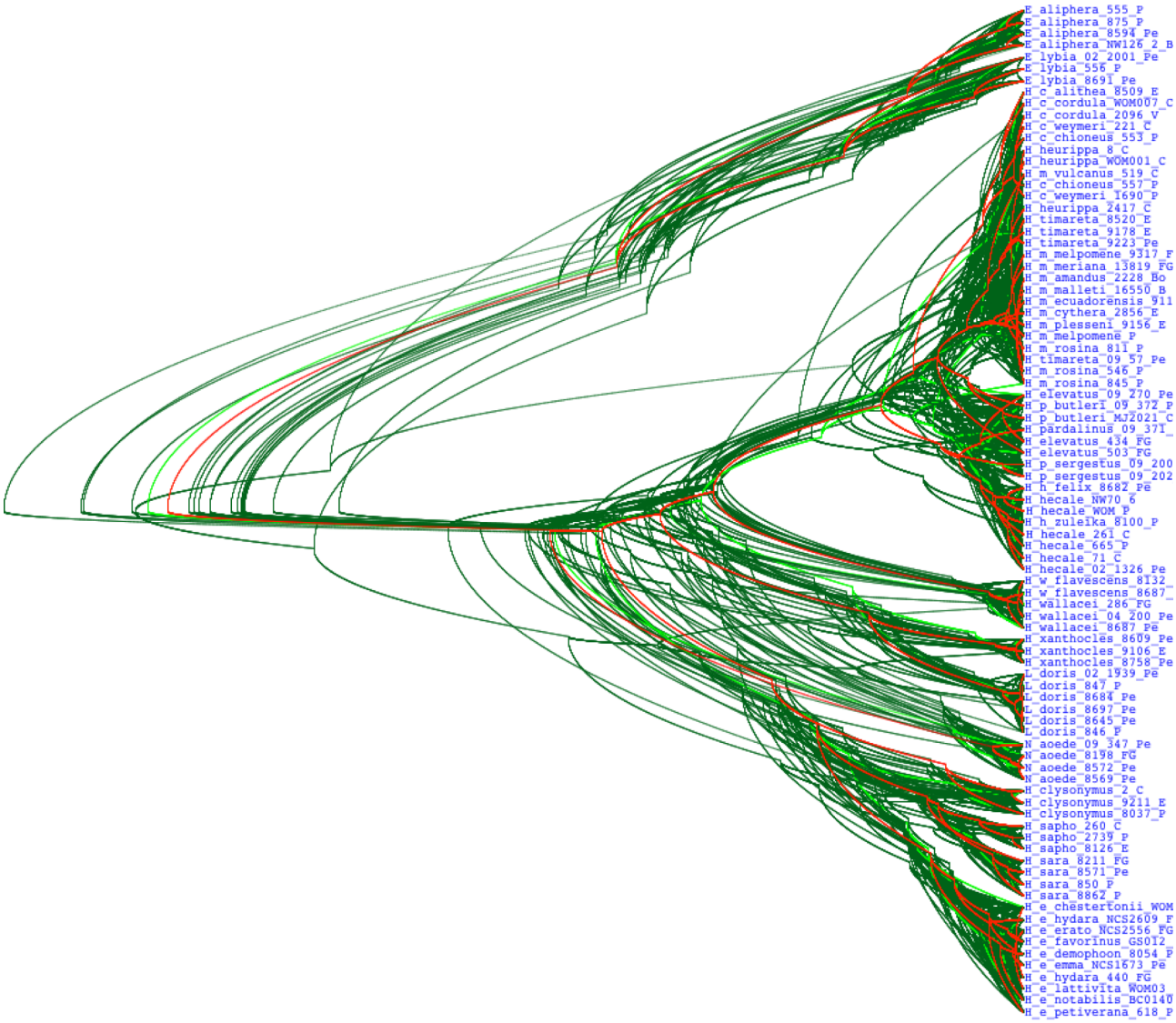

1416

1417 Supplementary Figure S1. Gene tree estimates for well-sampled *Heliconius* species from the Bayesian multispecies

1418 coalescent analysis in *BEAST. Reticulation reaches the highest levels in the *Heliconius melpomene* clade.

1419

1420

1421

1422

1423

1424

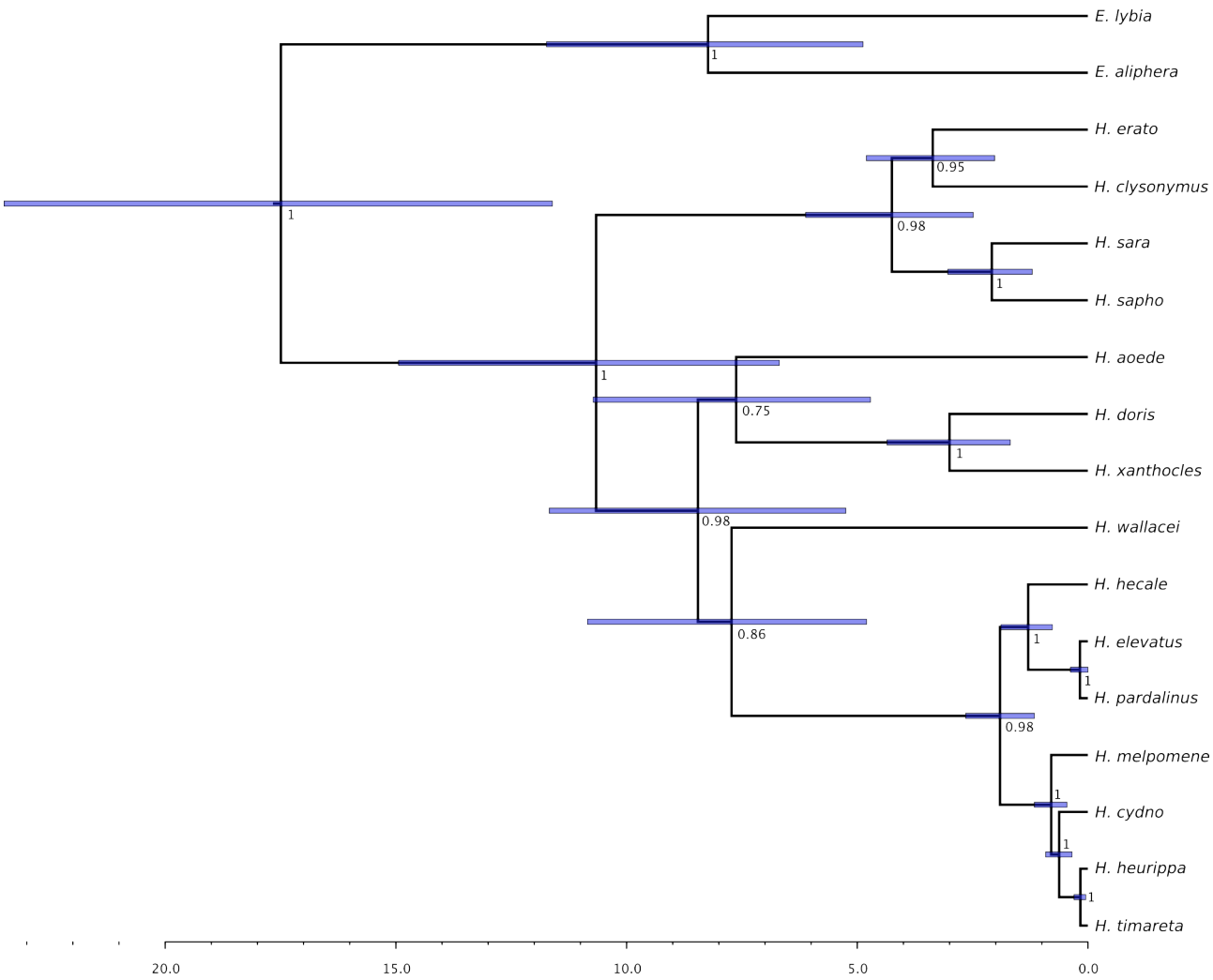

Supplementary Figure S2. Species tree from the *BEAST analysis. The times of divergence were estimated using a relaxed molecular clock with the prior on the mean age of the root based on a dating of the Nymphalidae radiation (Wahlberg et al. 2009). Node bars show the 95% confidence intervals around the mean age. The scale axis indicates time in Ma.

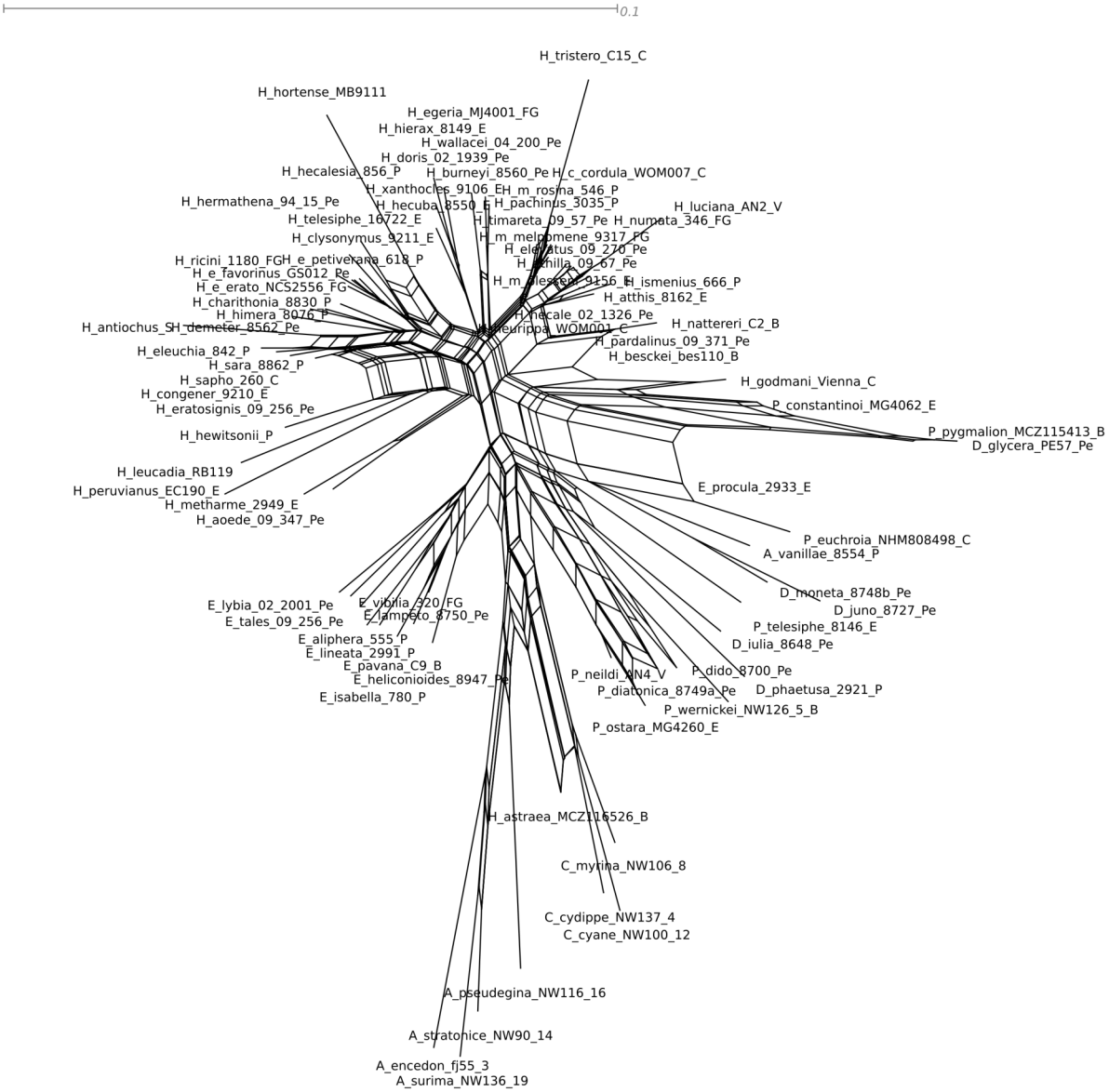

Supplementary Figure S3. NeighborNet network of Heliconiini based on pairwise DNA distances computed under the F84 model of sequence evolution in SplitsTree v.4. Reticulation is especially pronounced at the vertices linking genera and subgenera of *Heliconius*. The scale bar is in units of average number of substitutions per site.

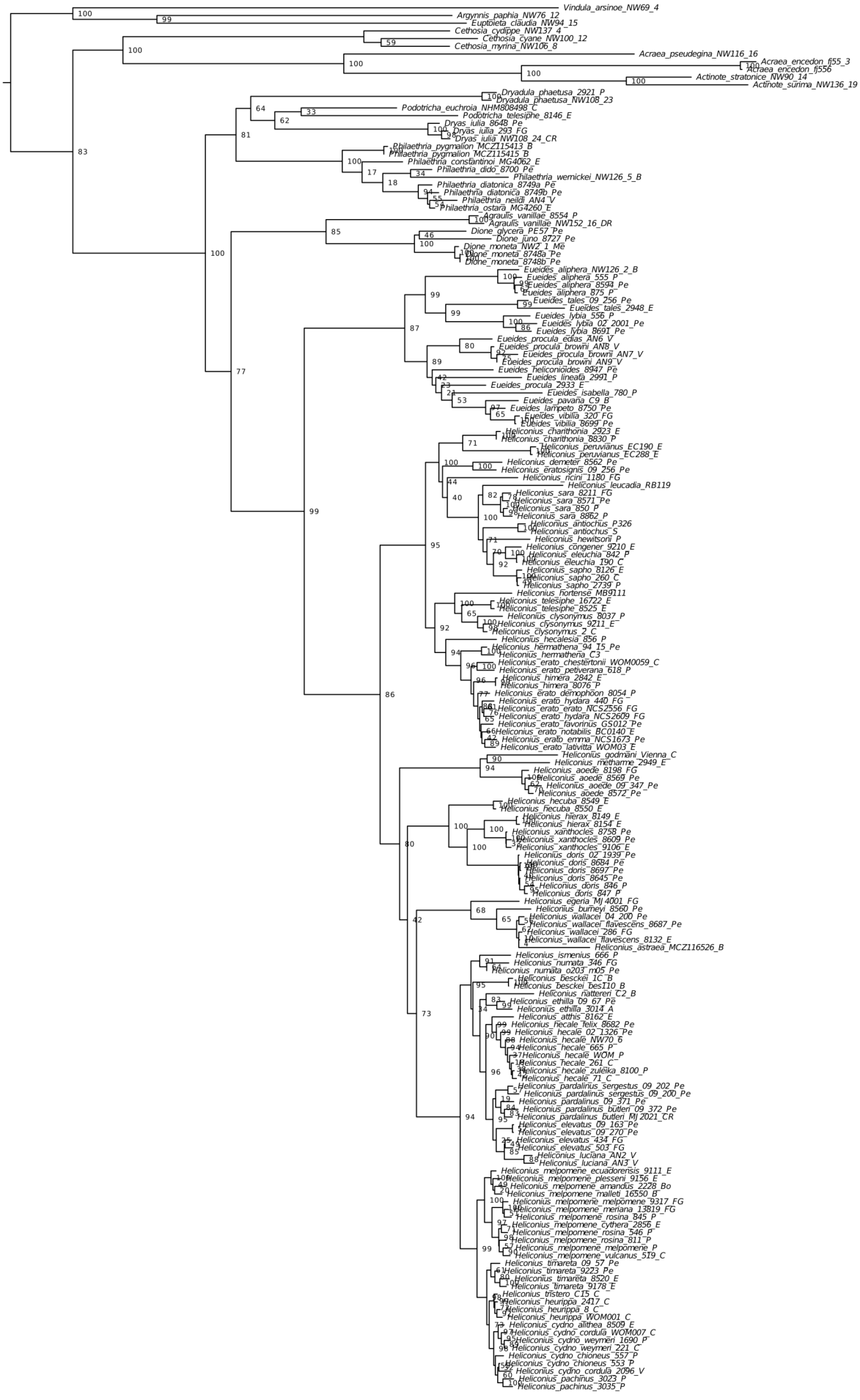
Vindula_arsinoe_NW69_4
Argynnis_paphia_NW76_12
Euptoieta_claudia_NW94_15
Cethosia_cydippe_NW137_4
Cethosia_cyane_NW100_12
Cethosia_myrina_NW106_8
Acraea_pseudegina_NW116_16
Acraea_encedon_fj55_3
Acraea_encedon_fj556
Actinote_stratonice_NW90_14
Actinote_surima_NW136_19
Dryadula_phaetusa_2921_P
Dryadula_phaetusa_NW108_23
Podotricha_euchroia_NHM808498_C
Podotricha_telesiphe_8146_E
Dryas_iulia_8648_Pe
Dryas_iulia_293_FG
Dryas_iulia_NW108_24_CR
Philaethria_pygmalion_MCZ115413_B
Philaethria_pygmalion_MCZ115415_B
Philaethria_constantinoi_MG4062_E
Philaethria_dido_8700_Pe
Philaethria_wernickei_NW126_5_B
Philaethria_diatonica_8749a_PE
Philaethria_diatonica_8749b_Pe
Philaethria_neildi_AN4_V
Philaethria_ostara_MG4260_E
Agraulis_vanillae_8554_P
Agraulis_vanillae_NW152_16_DR
Dione_glycera_PE57_Pe
Dione_juno_8727_Pe
Dione_moneta_NW2_1_Me
Dione_moneta_8748a_Pe
Dione_moneta_8748b_Pe
Eueides_aliphera_NW126_2_B
Eueides_aliphera_555_P
Eueides_aliphera_8594_Pe
Eueides_aliphera_875_P
Eueides_tales_09_256_Pe
Eueides_tales_2948_E
Eueides_lybia_556_P
Eueides_lybia_02_2001_Pe
Eueides_lybia_8691_Pe
Eueides_procula_edias_AN6_V
Eueides_procula_browni_AN8_V
Eueides_procula_browni_AN7_V
Eueides_procula_browni_AN9_V
Eueides_heliconioides_8947_Pe
Eueides_lineata_2991_P
Eueides_procula_2933_E
Eueides_isabella_780_P
Eueides_pavana_C9_B
Eueides_lampeto_8750_Pe
Eueides_vibilia_320_FG
Eueides_vibilia_8699_Pe
Heliconius_charithonia_2923_E
Heliconius_charithonia_8830_P
Heliconius_peruvianus_EC190_E
Heliconius_peruvianus_EC288_E
Heliconius_demeter_8562_Pe
Heliconius_eratosignis_09_256_Pe
Heliconius_ricini_1180_FG
Heliconius_leucadia_RB119
Heliconius_sara_8211_FG
Heliconius_sara_8571_Pe
Heliconius_sara_850_P
Heliconius_sara_8862_P
Heliconius_antiochus_P326
Heliconius_antiochus_S
Heliconius_hewitsonii_P
Heliconius_congener_9210_E
Heliconius_eleuchia_842_P
Heliconius_eleuchia_190_C
Heliconius_sapho_8126_E
Heliconius_sapho_260_C
Heliconius_sapho_2739_P
Heliconius_hortense_MB9111
Heliconius_telesiphe_16722_E
Heliconius_telesiphe_8525_E
Heliconius_clysonymus_8037_P
Heliconius_clysonymus_9211_E
Heliconius_clysonymus_2_C
Heliconius_hecalesia_856_P
Heliconius_hermathena_94_15_Pe
Heliconius_hermathena_C3
Heliconius_erato_chestertonii_WOM0059_C
Heliconius_erato_petiverana_618_P
Heliconius_himera_2842_E
Heliconius_himera_8076_P
Heliconius_erato_demophoon_8054_P
Heliconius_erato_hydara_440_FG
Heliconius_erato_erato_NCS2556_FG
Heliconius_erato_hydara_NCS2609_FG
Heliconius_erato_favorinus_GS012_Pe
Heliconius_erato_notabilis_BC0140_E
Heliconius_erato_emma_NCS1673_Pe
Heliconius_erato_lativitta_WOM03_E
Heliconius_godmani_Vienna_C
Heliconius_metharme_2949_E
Heliconius_aoede_8198_FG
Heliconius_aoede_8569_Pe
Heliconius_aoede_09_347_Pe
Heliconius_aoede_8572_Pe
Heliconius_hecuba_8549_E
Heliconius_hecuba_8550_E
Heliconius_hierax_8149_E
Heliconius_hierax_8154_E
Heliconius_xanthocles_8758_Pe
Heliconius_xanthocles_8609_Pe
Heliconius_xanthocles_9106_E
Heliconius_doris_02_1939_Pe
Heliconius_doris_8684_Pe
Heliconius_doris_8697_Pe
Heliconius_doris_8645_Pe
Heliconius_doris_846_P
Heliconius_doris_847_P
Heliconius_egeria_MJ_4001_FG
Heliconius_burneyi_8560_Pe
Heliconius_wallacei_04_200_Pe
Heliconius_wallacei_flavescens_8687_Pe
Heliconius_wallacei_286_FG
Heliconius_wallacei_flavescens_8132_E
Heliconius_astraea_MCZ116526_B
Heliconius_ismenius_666_P
Heliconius_numata_346_FG
Heliconius_numata_o203_m05_Pe
Heliconius_besckei_1C_B
Heliconius_besckei_besI10_B
Heliconius_hatterei_C2_B
Heliconius_ethilla_09_67_Pe
Heliconius_ethilla_3014_A
Heliconius_atthis_8162_E
Heliconius_hecale_felix_8682_Pe
Heliconius_hecale_02_1326_Pe
Heliconius_hecale_NW70_6
Heliconius_hecale_665_P
Heliconius_hecale_WOM_P
Heliconius_hecale_261_C
Heliconius_hecale_zuleika_8100_P
Heliconius_hecale_71_C
Heliconius_pardalinus_sergestus_09_202_Pe
Heliconius_pardalinus_sergestus_09_200_Pe
Heliconius_pardalinus_09_371_Pe
Heliconius_pardalinus_butleri_09_372_Pe
Heliconius_pardalinus_butleri_MJ2021_CR
Heliconius_elevatus_09_163_Pe
Heliconius_elevatus_09_270_Pe
Heliconius_elevatus_434_FG
Heliconius_elevatus_503_FG
Heliconius_luciana_AN2_V
Heliconius_luciana_AN3_V
Heliconius_melpomene_ecuadorensis_9111_E
Heliconius_melpomene_plesseni_9156_E
Heliconius_melpomene_amandus_2228_Bo
Heliconius_melpomene_malleti_16550_B
Heliconius_melpomene_melpomene_9317_FG
Heliconius_melpomene_meriana_13819_FG
Heliconius_melpomene_rosina_845_P
Heliconius_melpomene_cythera_2856_E
Heliconius_melpomene_rosina_346_P
Heliconius_melpomene_rosina_811_P
Heliconius_melpomene_melpomene_P
Heliconius_melpomene_vulcanus_519_C
Heliconius_timareta_09_57_Pe
Heliconius_timareta_9223_Pe
Heliconius_timareta_8520_E
Heliconius_timareta_9178_E
Heliconius_tristero_C15_C
Heliconius_heurippa_2417_C
Heliconius_heurippa_8_C
Heliconius_heurippa_WOM001_C
Heliconius_cydno_alithea_8509_E
Heliconius_cydno_cordula_WOM007_C
Heliconius_cydno_weymeri_1690_P
Heliconius_cydno_weymeri_221_C
Heliconius_cydno_chioneus_557_P
Heliconius_cydno_chioneus_553_P
Heliconius_cydno_cordula_2096_V
Heliconius_pachinus_3023_P
Heliconius_pachinus_3035_P
0.03

Supplementary Figure S4. Maximum Likelihood (RAxML) phylogeny of Heliconiini butterflies based on two mitochondrial and 20 nuclear genes, estimated under the GTR+G model. Support values are estimated based on 1000 bootstrap replicates. All specimens are included in this analysis. The scale bar is in units of average number of substitutions per site.

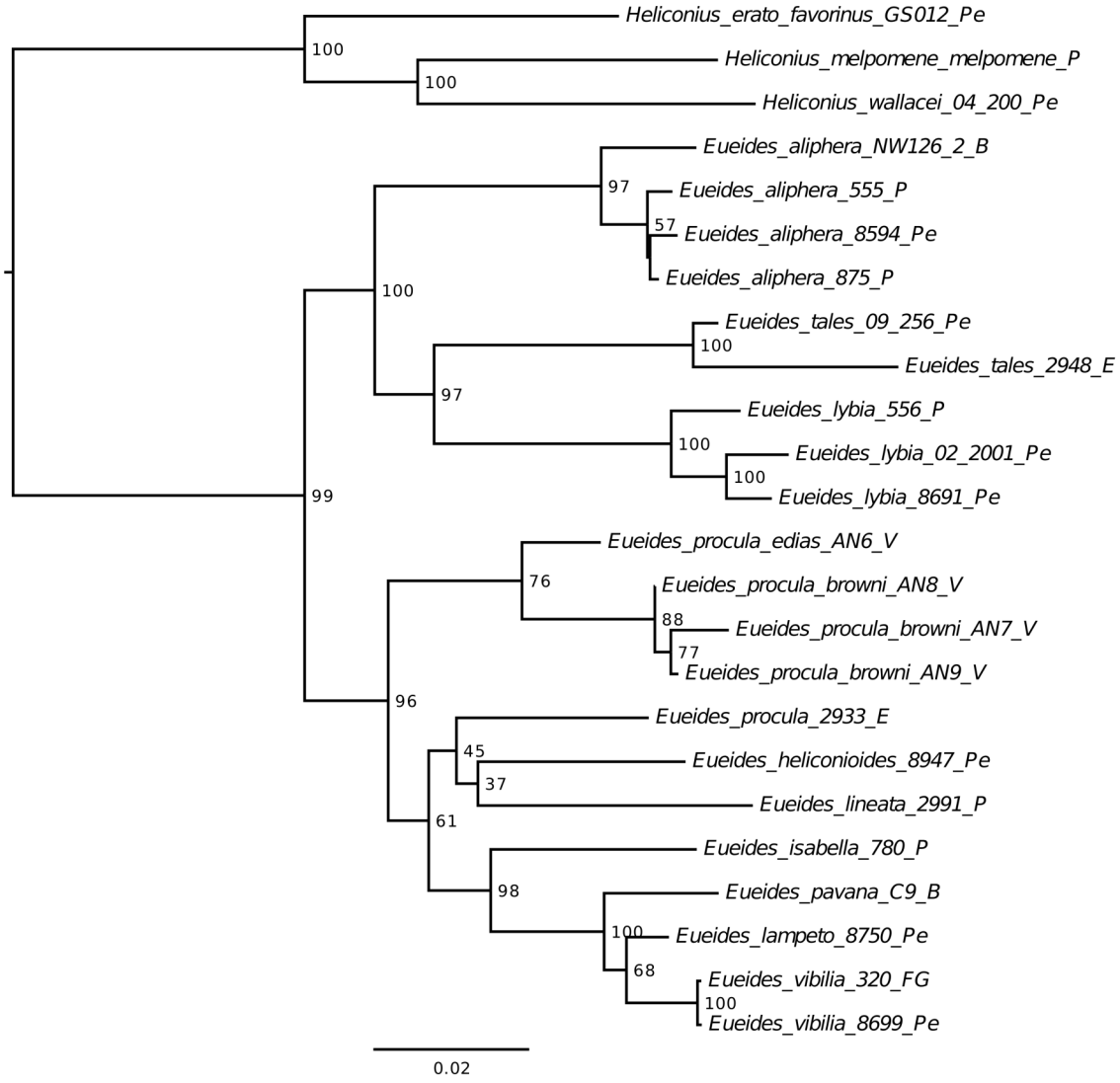

Supplementary Figure S5. Maximum Likelihood (RAxML, GTR+G model) phylogeny of the genus *Eueides* based on 11 loci sampled in most of the species. Support values based on 1000 bootstrap repliactes, scale bar is in units of average number of substitutions per site.

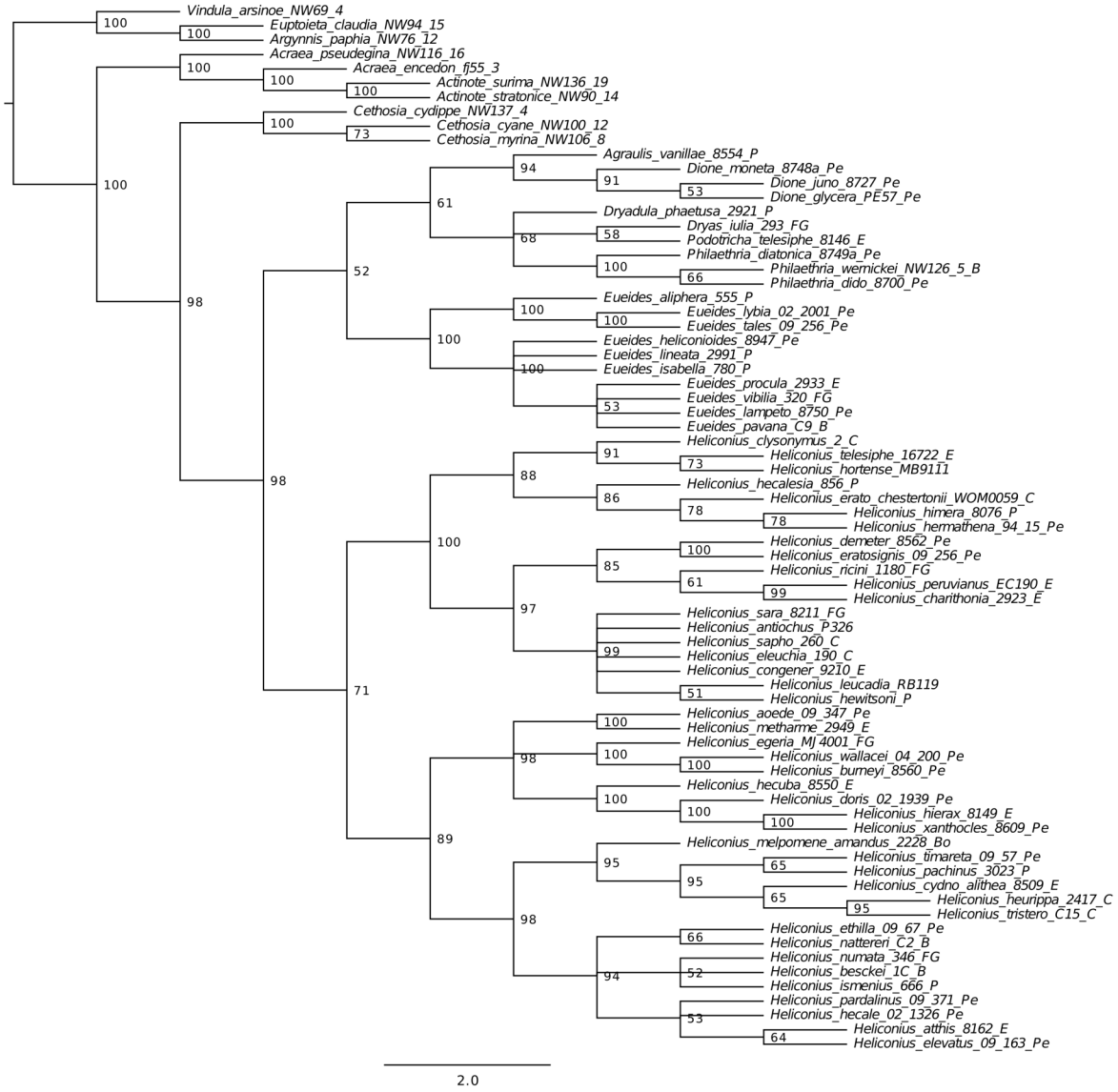

1485

1486 Supplementary Figure S6. Minimise deep coalescences (MDC) phylogeny of Heliconiini: a 50% consensus of 100

1487 bootstrap replicates of the set of 22 Bayesian gene trees.

1488